88. Supersymmetry, Part II (Experiment)

Revised August 2025 by M. D'Onofrio (Liverpool U.) and F. Moortgat (CERN; Ghent U.).

88.1 Introduction

Supersymmetry (SUSY), a transformation relating fermions to bosons and vice versa [1–9] is one of the most compelling possible extensions of the Standard Model of particle physics (SM).

On theoretical grounds SUSY is motivated as a generalization of space-time symmetries. A low-energy realization of SUSY, *i.e.*, SUSY at the TeV scale, is, however, not a necessary consequence. Instead, low-energy SUSY is motivated by the possible cancellation of quadratic divergences in radiative corrections to the Higgs boson mass [10–15]. Furthermore, it is intriguing that a weakly interacting, (meta)stable supersymmetric particle might make up some or all of the dark matter in the Universe [16–18]. In addition, SUSY GUTs predicts that gauge couplings, as measured experimentally at the electroweak scale, unify at an energy scale $\mathcal{O}(10^{16})$ GeV ("GUT scale") near the Planck scale [19–25].

In the minimal supersymmetric extension to the Standard Model, the so called MSSM [11,26,27]. a supersymmetry transformation relates every chiral fermion and gauge boson in the SM to a supersymmetric partner with half a unit of spin difference, but otherwise with the same properties (such as mass) and quantum numbers. The MSSM Higgs sector contains two doublets, which give mass to the up-type and down-type quarks, respectively. After electroweak symmetry breaking, five Higgs bosons arise, of which two are charged. The supersymmetric partners of chiral fermions are squarks (\tilde{q}) and sleptons $(\ell, \tilde{\nu})$, and the "gauginos" for gauge bosons. The supersymmetric partners of the Higgs doublets are known as "higgsinos." The weak gauginos and higgsinos mix, giving rise to charged mass eigenstates called "charginos" ($\tilde{\chi}^{\pm}$), and neutral mass eigenstates called "neutralinos" $(\tilde{\chi}^0)$. These are often collectively referred to as electroweakinos (EWkinos). The SUSY partners of the gluons are known as "gluinos" (\tilde{q}). The fact that such particles are not yet observed leads to the conclusion that, if supersymmetry is realized, it is a broken symmetry. A description of broken SUSY in the form of an effective Lagrangian with only "soft" SUSY breaking terms maintains the cancellation of quadratic divergences and furthermore if the SUSY particle masses are of order TeV, removes the need for large cancellations in the predicted Higgs vacuum expectation value.

The phenomenology of the MSSM is to a large extent defined by the interactions that bring SUSY breaking from the SUSY breaking sector to the MSSM, as well as the SUSY breaking scale. These determine the SUSY particle masses, the mass hierarchy, the field contents of physical particles, and their decay modes. In addition, phenomenology crucially depends on whether the multiplicative quantum number of R-parity [27], $R = (-1)^{3(B-L)+2S}$, where B and L are baryon and lepton numbers and S is the spin, is conserved or violated. If R-parity is conserved, SUSY particles (sparticles), which have odd R-parity, are produced in pairs and the decays of each SUSY particle must involve an odd number of lighter SUSY particles. The lightest SUSY particle (LSP) is then stable and often assumed to be a weakly interacting massive particle (WIMP). If R-parity is violated, new terms λ_{ijk} , λ'_{ijk} and λ''_{ijk} appear in the superpotential, where ijk are generation indices; λ -type couplings appear between lepton superfields only, λ'' -type are between quark superfields only, and λ' -type couplings connect the two. R-parity violation implies lepton and/or baryon number violation. More details of the theoretical framework of SUSY are discussed elsewhere in this volume [28].

The discovery of a Higgs boson with a mass around 125 GeV imposes constraints on SUSY models, which are discussed in Section 87. Low-energy data from flavor physics experiments,

high-precision electroweak observables as well as astrophysical data also impose strong constraints on the allowed SUSY parameter space. Recent examples of such data include measurements of the rare B-meson decay $B_s \to \mu^+\mu^-$ [29–31], measurements of the anomalous magnetic moment of the muon [32, 33], and accurate determinations of the cosmological dark matter relic density constraint [34, 35].

Indirect constraints can be more sensitive to higher SUSY mass scales than experiments searching for direct sparticle production at colliders, but the interpretation of these results is often strongly model dependent. In contrast, direct searches for sparticle production at collider experiments, which are the main topic of this review, are less subject to interpretation ambiguities and therefore they play a crucial role in the search for SUSY. Further discussion on indirect constraints can be found in 87.7.2.

88.2 Overview of the experimental search programme

The electron-positron collider LEP was operational at CERN between 1989 and 2000. In the initial phase, center-of-mass energies around the Z-peak were probed, but after 1995 the LEP experiments collected a significant amount of luminosity at higher center-of-mass energies, some 235 pb^{-1} per experiment at $\sqrt{s} \geq 204 \text{ GeV}$, with a maximum \sqrt{s} of 209 GeV. Searches for new physics at e^+e^- colliders benefit from the clean experimental environment and the fact that the initial state four-momentum is precisely known. This allows momentum balance to be exploited not only in the plane transverse to the beam but also along the beam direction (up to the small effects of beamstrahlung and the beam pipe holes). In contrast, at hadron colliders only the transverse momentum balance can be used, since the longitudinal momentum of the initial partons is not known on an event-by-event basis. Searches at LEP are dominated by the data samples taken at the highest center-of-mass energies.

The CDF and D0 experiments at the Tevatron, a proton-antiproton collider at a center-of-mass energy of up to 1.96 TeV, had an extensive search program for supersymmetric particles. CDF and D0 collected integrated luminosities between 10 and 11 fb⁻¹ each up to the end of collider operations in 2011.

The electron-proton collider HERA provided collisions to the H1 and ZEUS experiments between 1992 and 2007, at a center-of-mass energy up to 318 GeV. A total integrated luminosity of approximately 0.5 fb⁻¹ was collected by each experiment. At HERA, SUSY searches focused on R-parity violating processes mediated by λ' couplings, which allow resonant production of single squarks in electron–quark interactions.

The Large Hadron Collider (LHC) at CERN started proton-proton operation at a center-of-mass energy of 7 TeV in 2010. By the end of 2011 the ATLAS and CMS experiments had collected about 5 fb⁻¹ of integrated luminosity each, and the LHCb experiment had collected approximately 1 fb⁻¹. In 2012, the LHC operated at a center-of-mass energy of 8 TeV, and ATLAS and CMS collected approximately 20 fb⁻¹ each, whereas LHCb collected 2 fb⁻¹. In 2015, the LHC started Run 2, with a center-of-mass energy of 13 TeV. At the end of Run 2 in November 2018, ATLAS and CMS had both collected approximately 140 fb⁻¹, and LHCb had collected almost 6 fb⁻¹. The Run 3 of the LHC started in July 2022 with a center-of-mass energy of 13.6 TeV. Almost 240 fb⁻¹ of data have been collected by ATLAS and CMS at the time of writing (August 2025), and LHCb collected around 90 fb⁻¹.

At the LHC, cross sections of QCD-mediated processes are the largest achievable at colliders, which is reflected in the higher sensitivity for SUSY particles carrying color charge, squarks and gluinos, with respect to LEP, Tevatron and HERA. In particular, proton-proton collisions at the LHC differ from proton-antiproton collisions at the Tevatron as there are no valence anti-quarks in the proton, and that gluon-initiated processes play a more dominant role. The increased center-

of-mass energy of the LHC compared to the Tevatron significantly extends the kinematic reach for SUSY searches. This is reflected foremost in the sensitivity for squarks and gluinos, but also for SUSY particles produced via electroweak processes.

In this review we report results of direct searches for SUSY particles at colliders up to August 2023, mostly covering data analyses at the ATLAS and CMS experiments with reference to results from LEP, HERA and the Tevatron. For more details on LEP and Tevatron constraints, see earlier PDG reviews [36]. Analyses on the Run 3 datasets are still in progress hence the results reported for ATLAS and CMS are mostly based on Run 2 data. Results are categorized depending on the targeted SUSY particles, the nature of their production and decays, and the assumption on *R*-parity. Brief summaries of search techniques and approaches adopted for interpretation of the results are given in Section 88.3 and 88.4, respectively. Sections 88.5-88.8 focus on results for promptly-decaying gluinos and first and second generation squarks, top and bottom squarks, electroweakinos (charginos, neutralinos) and sleptons. Limits obtained for sparticle masses assuming *R*-parity violating models are also reported. Results of dedicated searches for long-lived (LL) SUSY particles are reported in Section 88.9. Finally, Section 88.10 provides examples of global reinterpretations of SUSY searches.

88.3 Experimental search techniques

Large background contributions from Standard Model processes pose challenges to the trigger and analysis. Such backgrounds are dominated by multijet production processes, including, particularly at the LHC, those of top quark production, as well as jet production in association with vector bosons. The proton's momentum is shared between its parton constituents, and in each collision only a fraction of the total center-of-mass energy is available in the hard parton-parton scattering. Since the parton momenta in the longitudinal direction are not known on an event-by-event basis, use of momentum conservation constraints in an analysis is restricted to the transverse plane, leading to the definition of transverse variables, such as the missing transverse momentum, and the transverse mass.

Under the assumption of R-parity conservation (RPC), the typical SUSY search signature for squarks and gluinos at hadron colliders contains high- $p_{\rm T}$ jets, which are produced in the decay chains of heavy squarks and gluinos, and significant missing transverse momentum originating from the two LSPs produced at the end of the decay chains, which escape experimental detection. Electroweakino decays are often characterised by the presence of leptons, for instance from W and Z bosons in the decay chain, plus missing transverse momentum. Standard Model backgrounds with missing transverse momentum include leptonic W/Z-boson decays, associated production of jets and a Z-boson decaying into neutrinos, semi-leptonic heavy-flavor decays to neutrinos, top-quark pair production with one or both W bosons decaying leptonically, and multijet events that may be affected by instrumental effects such as jet mis-measurement.

Selection variables designed to separate the SUSY signal from the Standard Model backgrounds include transverse variables such as $H_{\rm T}$, $E_{\rm T}^{\rm miss}$, and $m_{\rm eff}$. The quantities $H_{\rm T}$ and $E_{\rm T}^{\rm miss}$ refer to the measured transverse energy and the missing transverse momentum in the event, respectively. They are usually defined as the scalar sum of the transverse jet momenta or of the transverse energies of calorimeter clusters measured in the event $(H_{\rm T})$, or the magnitude $(E_{\rm T}^{\rm miss})$ of the negative vector sum of transverse momenta of reconstructed objects like jets and leptons in the event $(\bar{p}_{\rm T}^{\rm miss})$. The quantity $m_{\rm eff}$ is referred to as the effective mass of the event and is defined as $m_{\rm eff} = H_{\rm T} + E_{\rm T}^{\rm miss}$. The peak of the $m_{\rm eff}$ distribution for SUSY signal events correlates with the SUSY mass scale, in particular with the produced sparticle masses and the mass difference between the primary produced SUSY particle and the LSP [37], whereas the Standard Model backgrounds dominate at low $m_{\rm eff}$. An additional reduction of multijet backgrounds can be achieved by demanding isolated

leptons or photons in the final states; in such events the lepton or photon transverse momentum may be added to $H_{\rm T}$ or $m_{\rm eff}$ for further signal-background separation. Other kinematic variables and approaches developed to increase the sensitivity to pair production of heavy sparticles with TeV-scale masses focusing on the kinematics of their decays are the $\alpha_{\rm T}$ [38–42], razor [43], stransverse mass ($m_{\rm T2}$) [44], and contransverse mass ($m_{\rm CT}$) [45] variables. The super-razor [46] and recursive jigsaw reconstruction [47] techniques are topological event reconstruction methods also used in searches for sparticles with masses in the TeV-range. In case massive, unstable SM particles such as top quarks, vector bosons or the Higgs boson arise in the decay chain, dedicated procedures are employed for their reconstruction and identification. If these are produced with a significant boost, their decay products will typically overlap and become collimated (boosted) in the direction of the parent particle. Their hadronic decay products can be reconstructed as a single large-radius jet (see studies from ATLAS [48]), and jet-substructure [49] techniques can be adopted. Machine-learning (ML) approaches are also used to identify and classify hadronic decays of highly Lorentz-boosted bosons and top quarks, see as example recent studies from CMS [50].

Until recently, analyses used simple combinations of selections on kinematic variables (often referred to as *cut-and-count* analyses) and exploited multiple signal regions defined by categorizing events on the basis of several variables and their correlations. An example is provided in Fig. 88.1 from Ref. [51]: 39 signal regions are set to search for top squarks in events with one lepton, jets and missing transverse momentum. Regions depend on jet multiplicities, reconstructed top-quark candidates and thresholds applied to the most discriminant variables used for optimisation.

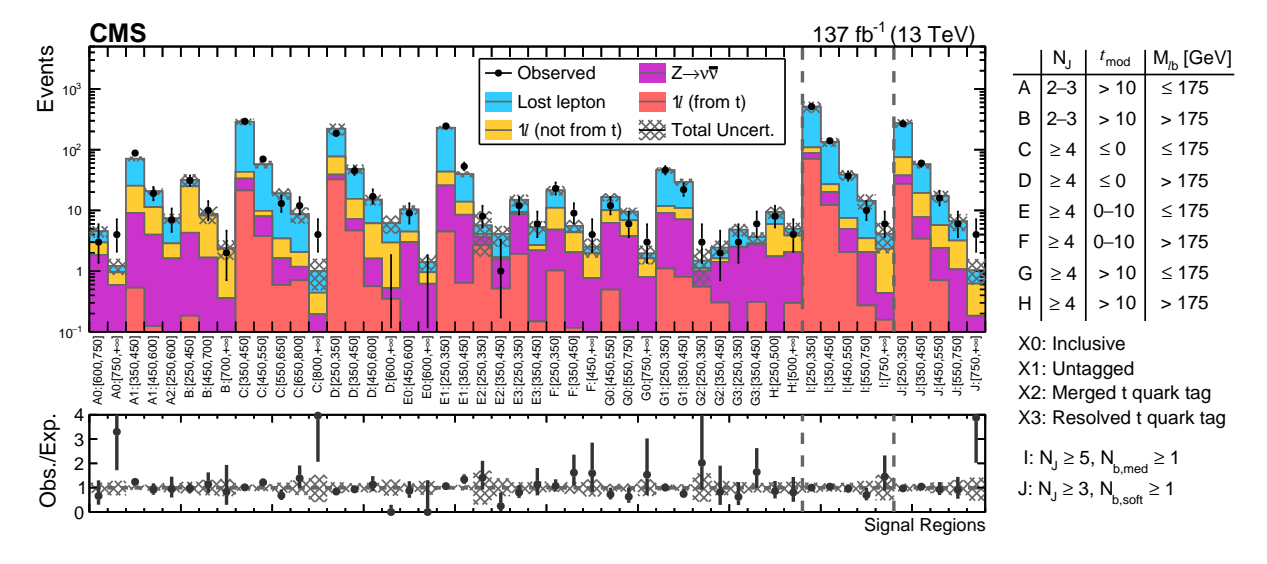


Figure 88.1: Example of multiple signal regions set for a typical SUSY search at the LHC. For definition of regions and acronyms specific for this search, see corresponding paper.

At present, shape analyses or analyses using more sophisticated techniques, e.g. machine learning, are being developed more and more often. ML techniques allow analyses to better capture the complexity of the events and achieve improved sensitivity with respect to counting experiments. For example, Boosted Decision Trees (BDTs) allow analyses to exploit simultaneously the discriminating power of multiple variables and that of correlations among objects in the events. Deep Neural Networks (NN) are also employed for object reconstruction and to use directly detector-recorded energies and momenta of produced particles instead of first deriving a restricted set of physical variables. Among others, currently in use are Convolutional NN for image classification techniques, Recurrent NN, parametric NN, Graph NN and Generative Adversarial Networks.

Variables and approaches reported above are also used in searches for R-parity violating (RPV) SUSY models where signal events are often characterised by the presence of multiple leptons and/or jets, and little or no missing transverse momentum. However, if R-parity violating couplings are small, sparticles might be long-lived and may travel macroscopic distances before decaying. Similarly, long lifetimes may be due to small mass splittings, as in the case of pure higgsino/wino scenarios, or to heavy mediators, as in Split SUSY models [52,53]. The identification of long-lived particles requires dedicated tools and their signatures can be very diverse. At the LHC, customized techniques (also based on NN) have been developed, for example, to reconstruct significantly displaced decay vertices or short track segments, and to identify tracks with atypical properties or unusual ionization, small and localized deposits of energy inside of the calorimeters without associated tracks, or stopped particles that decay out of time with collisions. For an overview, see Ref. [54].

88.4 Interpretation of search results

Since the mechanism by which SUSY is broken is unknown, a general approach to SUSY via the most general soft SUSY breaking Lagrangian adds a significant number of new free parameters. For the minimal supersymmetric standard model, MSSM, *i.e.*, the model with the minimal particle content, these comprise 105 new real degrees of freedom. A phenomenological analysis of SUSY searches leaving all these parameters free is not feasible. For the practical interpretation of SUSY searches at colliders several approaches are taken to reduce the number of free parameters.

One approach is to assume a SUSY breaking mechanism and lower the number of free parameters through the assumption of additional constraints. Before the start of the LHC, interpretations of experimental results were often performed in constrained models of gravity mediated [55,56], gauge-mediated [57–59], and anomaly mediated [60,61] SUSY breaking. The most popular model was the constrained MSSM (CMSSM) [55,62,63], which in the literature is also referred to as minimal supergravity, or MSUGRA. These constrained SUSY models are theoretically well motivated and provide a rich spectrum of experimental signatures. However, with universality relations imposed on the soft SUSY breaking parameters, they do not cover all possible kinematic signatures and mass relations of SUSY. Furthermore, the Higgs mass measurement from LHC Run 1, together with other collider and non-collider measurements, substantially limits the allowed SUSY parameter space for these models. This indicates that very constrained models like the CMSSM are no longer good benchmark scenarios to solely characterize the results of SUSY searches at the LHC and efforts have been made to complement them with more flexible approaches.

A broader and more comprehensive subset of the MSSM can be studied via the so-called phenomenological-MSSM, or pMSSM [64-67]. It is derived from the MSSM, using experimental data to eliminate parameters that are free in principle but have already been highly constrained by measurements of e.g., flavor mixing and CP-violation. This effective approach reduces the number of free parameters in the MSSM to typically 19 or even less, making it a practical compromise between the full MSSM and highly constrained models such as the CMSSM.

Even less dependent on fundamental assumptions are interpretations in terms of so-called simplified models [68–71]. Such models assume a limited set of SUSY particle production and decay modes and leave open the possibility to vary masses and other parameters freely. Therefore, simplified models enable comprehensive studies of individual SUSY topologies, and are useful for optimization of the experimental searches over a wide parameter space without limitations on fundamental kinematic properties such as masses and decay modes.

As a consequence, ATLAS and CMS have adopted simplified models as the primary framework to provide interpretations of their searches. In addition to using simplified models that describe prompt decays of SUSY particles, the experiments are now also focusing more on the use of simpli-

fied models that allow for decays of long-lived SUSY particles as they can arise in different SUSY scenarios (see Section 88.9 for further discussion). Today, almost every individual search provides interpretations of their results in one or several simplified models that are characteristic of SUSY topologies probed by the analysis.

While simplified models are very convenient for the interpretation of individual SUSY production and decay topologies, care must be taken when applying these limits to more complex SUSY spectra. In particular, the branching ratio of SUSY particles into a specific final state is often assumed to be 100% and in many of the quoted limits the LSP is assumed to be massless. Therefore, simplified model limits should be seen as an approximation of the constraints that can be placed on sparticle masses in more complex SUSY spectra. Only on a case-by-case basis can it be determined whether the limit of a given simplified model represents a good approximation of the true underlying constraint that can be applied on a sparticle mass in a complex SUSY spectrum. In the following, we will point out explicitly the assumptions that have entered the limits when quoting interpretations from simplified models.

Since none of the searches performed so far have shown significant excess above the SM background prediction, the interpretations of the presented results are exclusion limits on SUSY parameter space. Unless stated differently, all quoted exclusion limits are at the 95% confidence level. Finally, we note that many of the recent publications by ATLAS and CMS also present results in terms of model-independent limits such that their discovery potential is statistically quantified independently on a particular model.

88.5 Exclusion limits on gluino, first and second generation squark masses in RPC scenarios

Colored SUSY particles such as squarks and gluinos are produced via the strong interaction and have the highest cross sections at hadron colliders. Limits on squark masses of the order 100 GeV have been set by the LEP experiments [72], in the decay to quark plus neutralino, and for a mass difference between squark and quark plus neutralino of typically at least a few GeV. However, hadron collider experiments are able to set much more stringent mass limits.

The main production mechanisms at hadron colliders are squark-squark, squark-gluino and gluino-gluino production; when "squark" is used "antisquark" is also implied. Pair production usually involves both the s-channel and t-channel parton-parton interactions. However, since there is a negligible amount of bottom and top quark content in the proton, top and bottom squark production proceeds through s-channel diagrams only. Experimental analyses of squark and/or gluino production typically assume the first and second generation squarks to be approximately degenerate in mass. Cross section calculations at the center-of-mass energy of 13 TeV shown in Fig. 88.2 (from Ref. [73]) assume mass degeneracy of left- and right-handed u, d, s, c squarks. Other sparticle masses are considered decoupled, i.e, their masses are assumed to have a very high value (above or of the order of 10 TeV). The LHC experiments also provide simplified model limits on individual first or second generation squarks. Top and bottom squarks have the same production cross section, identical to that of a single light squark.

In this section, we focus on results assuming R-parity conservation. Limits set by the Tevatron experiments on the gluino mass assume the framework of the CMSSM, with $\tan \beta = 5$ (CDF) or $\tan \beta = 3$ (D0). Furthermore, the common trilinear term A_0 is set to 0 and the higgsino mass term μ is assumed to be less than 0. The resulting lower mass limits are about 310 GeV for all squark masses, or 390 GeV for the case $m_{\tilde{q}} = m_{\tilde{q}}$ [74,75].

ATLAS and CMS limits on the gluino mass have been established in the framework of simplified models. Assuming only gluino pair production, three main primary decay chains of the gluino have been considered by the LHC experiments for interpretations of their search results. The first decay

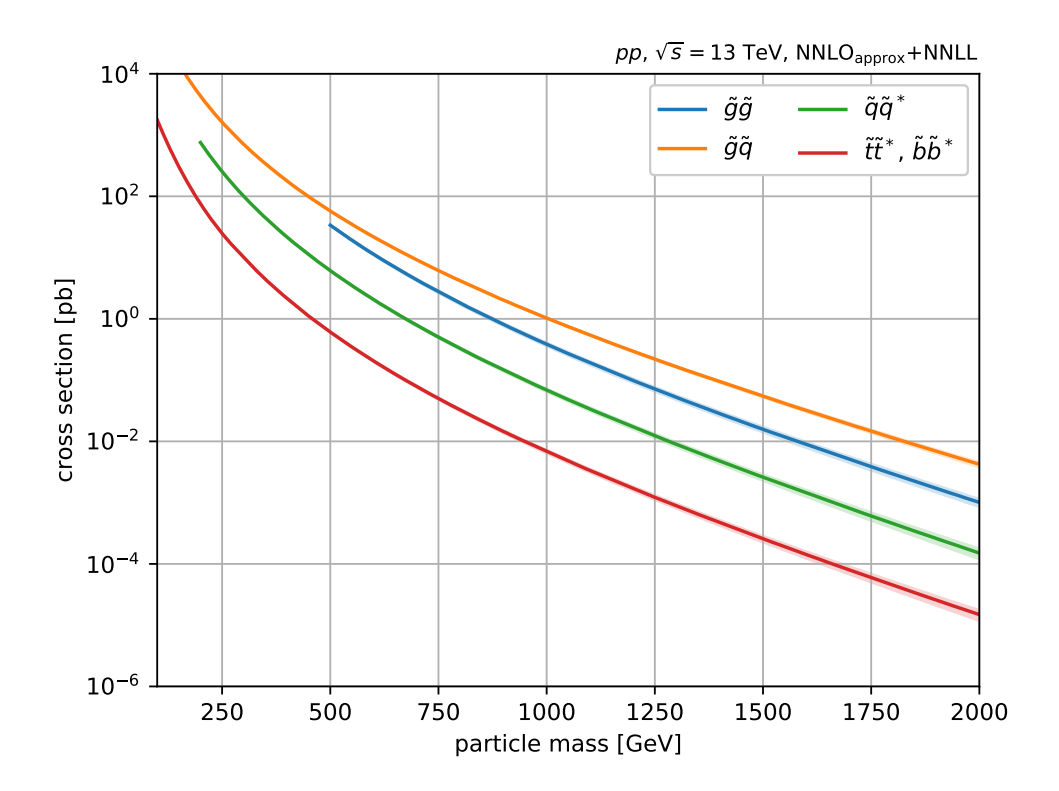


Figure 88.2: Cross sections for pair production of gluinos and squarks as a function of their mass at the LHC for a center-of-mass energy of 13 TeV. They are calculated at approximately next-to-next-to-leading-order (NNLO) including the resummation of soft gluon emission at the next-to-next-to-leading logarithmic accuracy.

chain, $\tilde{g} \to q\bar{q}\tilde{\chi}_1^0$, assumes gluino mediated production of first and second generation squarks (onshell or off-shell) which leads to four light flavor quarks in the final state. Therefore, inclusive all-hadronic analyses searching for multijet plus $E_{\mathrm{T}}^{\mathrm{miss}}$ final states are utilized to put limits on this simplified model. These limits are derived as a function of the gluino and neutralino (LSP) mass. As shown in Fig. 88.3 (left)the CMS collaboration [76] excludes in this simplified model gluino masses below approximately 2.1 TeV for a light neutralino mass below about 600 GeV. In scenarios where neutralinos are not very light, the efficiency of the analyses is reduced by the fact that jets are less energetic, and there is less missing transverse momentum in the event. This leads to weaker limits when the mass difference $\Delta m = m_{\tilde{g}} - m_{\tilde{\chi}_{\tilde{q}}}$ is reduced. For example, for neutralino masses above about 1.2 TeV no limit on the gluino mass can be set for this decay chain. Therefore, limits on gluino masses are strongly affected by the assumption of the neutralino mass. Similar results for this simplified model have been obtained by ATLAS [77]. A second simplified model postulates a decay chain where $\tilde{g} \to q\bar{q}W\tilde{\chi}_1^0$, assuming that the intermediate (on-shell or off-shell) squark is left-handed and decays to a chargino and a quark, with the chargino decaying to a Wboson and the LSP. This leads to two W bosons and four light flavor quarks plus $E_{\rm T}^{\rm miss}$ in the final state. Both leptonic and hadronic decays of the W can be considered. In this scenario, the ATLAS collaboration [78,79] excludes gluino masses below approximately 2.2 TeV for a sufficiently light neutralino and assuming the chargino mass is halfway between the gluino and neutralino mass, see Fig. 88.3 (right). Again, for neutralino masses above about 1.2 TeV, there exists no limit on the gluino mass for this decay chain. A similar reach has been obtained by the CMS collaboration [80, 80, 81], where the most recent results are obtained using novel algorithms based on deep neutral networks that identify hadronically decaying W bosons.

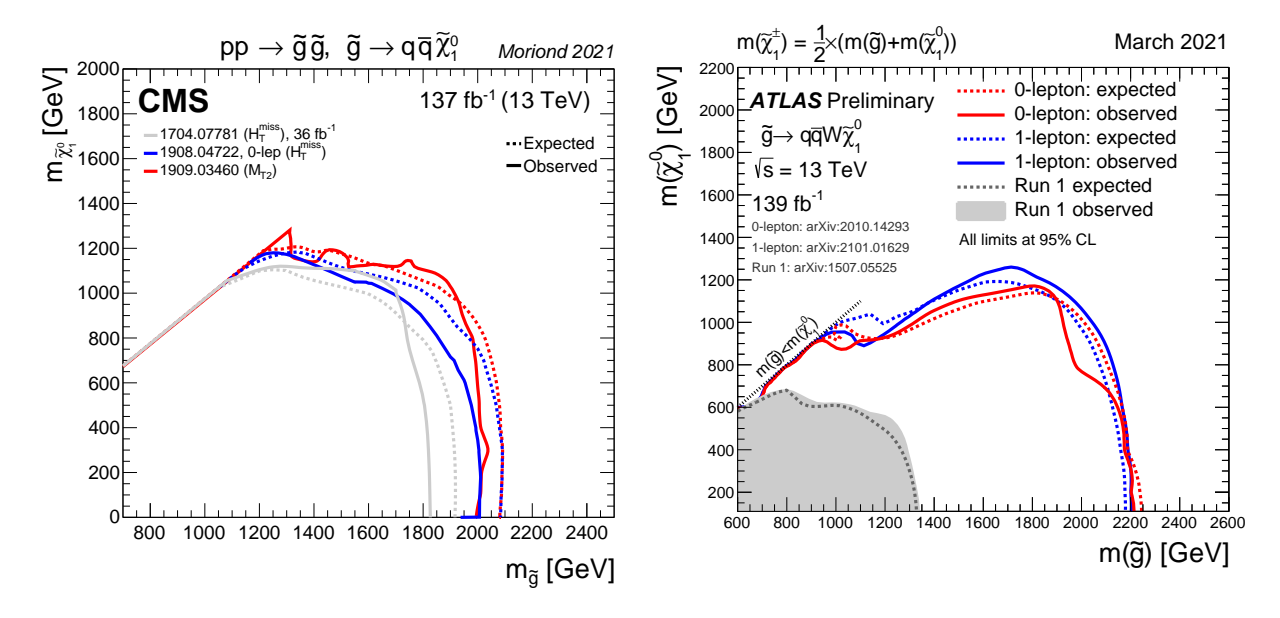


Figure 88.3: Lower mass limits, at 95% C.L., on gluino pair production for various decay chains in the framework of simplified models. Left: $\tilde{g} \to q\bar{q}\tilde{\chi}_1^0$, result of the CMS collaboration. Right: $\tilde{q} \to q\bar{q}W\tilde{\chi}_1^0$, result of the ATLAS collaboration.

Gluino decays are not limited to first and second generation squarks: another important decay chain of the gluino considered for interpretation in simplified models is $\tilde{g} \to b\bar{b}\tilde{\chi}_1^0$. In this case the decay is mediated via bottom squarks and thus leads to four jets originating from b-quarks and $E_{\rm T}^{\rm miss}$ in the final state. For this topology as well, inclusive all-hadronic searches provide the highest sensitivity. In this case, the use of secondary vertex reconstruction for the identification of jets originating from the b-quarks in the event provides a powerful handle to reject SM background contributions. Therefore, in addition to a multijet plus $E_{\rm T}^{\rm miss}$ signature these searches also require between 1 and 4 jets to be tagged as b-jets. As shown in Fig. 88.4 (left), for this simplified model CMS [76] excludes gluino masses below ≈ 2.3 TeV for a sufficiently light neutralino, while for neutralino masses above ≈ 1.5 TeV no limit on the gluino mass can be set. Comparable limits for this simplified model are provided by searches from ATLAS [82,83], with the most recent results pushing the boundary of gluino masses to 2.44 TeV in the case of a massless neutralino.

If kinematically allowed, decays of gluinos to top squarks via $\tilde{g} \to \tilde{t}t$ are also possible. This defines the next important simplified model characterizing gluino pair production, $\tilde{g} \to t\bar{t}\tilde{\chi}_1^0$, which leads to a "four tops" final state, $tttt\tilde{\chi}_1^0\tilde{\chi}_1^0$. The topology of this decay is very rich in different experimental signatures: as many as four isolated leptons, four *b*-jets, as many as eight light flavor quark jets, and significant missing transverse momentum from the neutrinos in the W decay and from the two neutralinos. As shown in Fig. 88.4 (right), the ATLAS search [82] rules out gluinos with masses below ≈ 2.4 TeV for light neutralinos in this model. For neutralino masses above ≈ 1.4 TeV, no limit can be placed on the gluino mass. Sensitivity is also achieved in case of gluino pairs with an off-shell top quark in the decay.

The CMS multiple b-jet search [84] and the search in full-hadronic events using identification techniques for boosted top-quarks in the final state [85] result in gluino mass limits of ≈ 2.3 TeV.

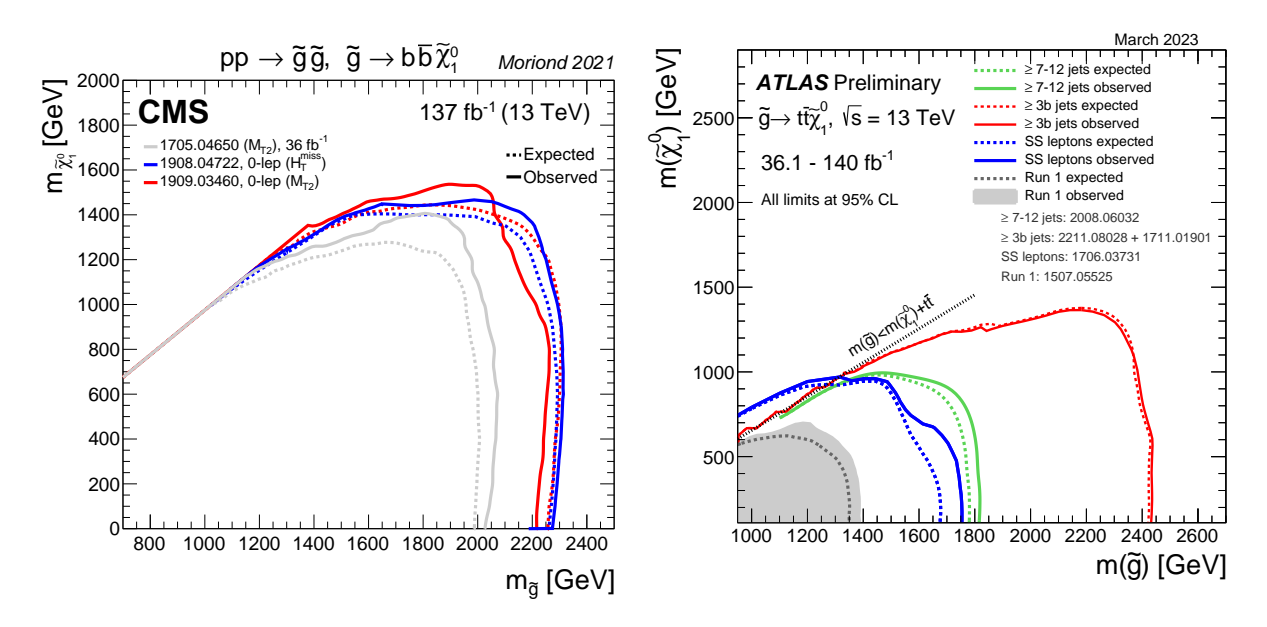


Figure 88.4: Lower mass limits, at 95% C.L., on gluino pair production for various decay chains in the framework of simplified models. Left: $\tilde{g} \to b\bar{b}\tilde{\chi}^0_1$. Right: $\tilde{g} \to t\bar{t}\tilde{\chi}^0_1$. Results from the CMS and ATLAS collaborations.

Assuming gluinos to be heavier than squarks, squarks will predominantly decay to a quark and a neutralino or chargino, if kinematically allowed. The decay may involve the lightest neutralino (typically the LSP) or chargino, but, depending on the masses and couplings of the gauginos and on the handedness of the squarks, may involve heavier neutralinos or charginos. For pair production of first and second generation squarks, the simplest decay modes involve two jets and missing transverse momentum, with potential extra jets stemming from initial state or final state radiation (ISR/FSR) or from decay modes with longer decay chains (cascades). In cascades, isolated photons or leptons may appear from the decays of sparticles such as neutralinos or charginos.

Limits on first and second generation squark masses set by the Tevatron experiments assume the CMSSM, and amount to lower limits of about 380 GeV for all gluino masses, or 390 GeV for the case $m_{\tilde{q}} = m_{\tilde{g}}$ [74,75]. At the LHC, limits on squark masses have been set using up to approximately 140 fb⁻¹ of data at 13 TeV. Interpretations in simplified models typically characterize squark pair production considering only one decay chain at the time for the squark, for instance $\tilde{q} \to q \tilde{\chi}_1^0$. It is usually assumed that the left and right-handed \tilde{u} , \tilde{d} , \tilde{s} and \tilde{c} squarks are degenerate in mass. Furthermore, it is assumed that the mass of the gluino is very high (above or order of 10 TeV) and thus contributions of the corresponding t-channel diagrams to squark pair production are negligible. Therefore, the total production cross section for this simplified model is eight times the production cross section of an individual squark (e.g. \tilde{u}_L). Under these assumptions, CMS obtains a lower squark mass limit of ≈ 1.75 TeV for light neutralinos [84], as shown in Fig. 88.5 (left). Only for neutralino masses below ≈ 800 GeV can any squark masses be excluded. Searches for new physics in monojet channels are sensitive to very compressed scenarios, and masses up to 900 GeV are excluded for $\Delta m = m_{\tilde{q}}, m_{\tilde{\chi}_1^0} \approx 5$ GeV [86].

If the assumption of mass degenerate first and second generation squarks is dropped and only the production of a single light squark is assumed, the limits weaken significantly. For example, the CMS limit on degenerate squarks of 1750 GeV for light neutralinos drops to ≈ 1300 GeV for pair production of a single light squark, and for neutralinos heavier than ≈ 600 GeV no squark

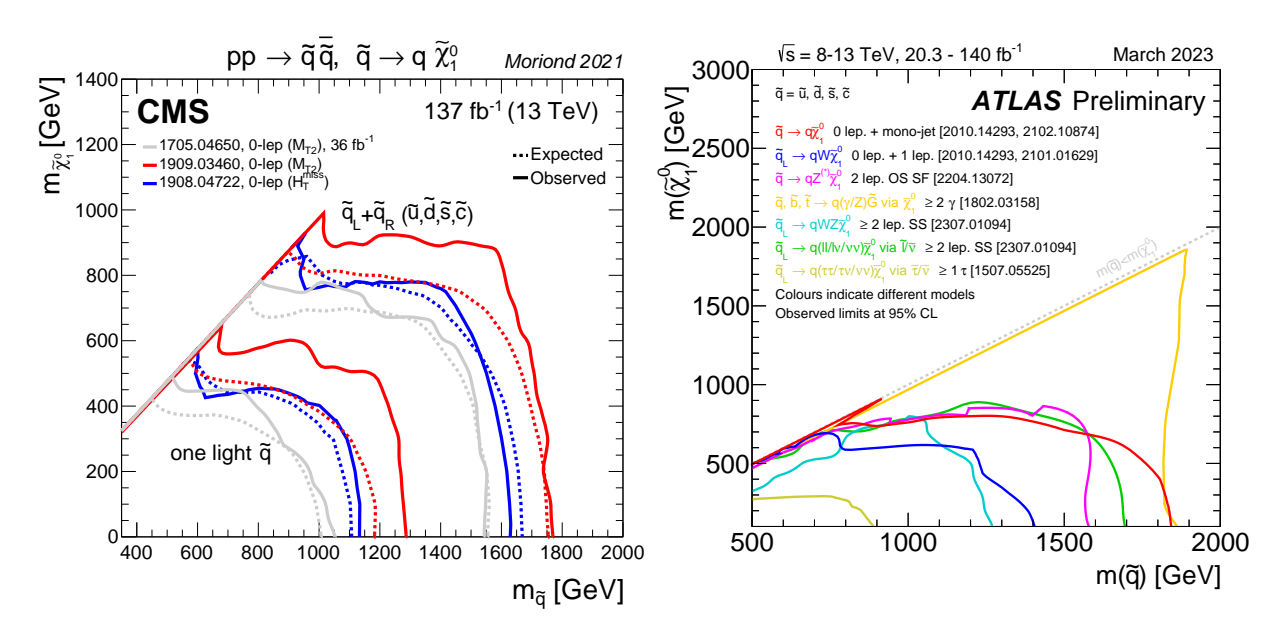


Figure 88.5: Left: 95% C.L. exclusion contours in the framework of simplified models assuming a single decay chain of $\tilde{q} \to q\tilde{\chi}_1^0$, obtained by the CMS collaboration. Right: Assuming more complicated decay chains including W or Z bosons, obtained by the ATLAS collaboration.

mass limit can be placed. It should be noted that this limit is not a result of a simple scaling of the above mentioned mass limits assuming eight-fold mass degeneracy but it also takes into account that for an eight times lower production cross section the analyses must probe kinematic regions of phase space that are closer to the ones of SM background production.

A summary of results of the ATLAS searches also targeting more complicated decay chains, where e.g. intermediate bosons are produced as well, can be seen in Fig. 88.5 (right). Depending on the topology, the exclusion limit can reach up to ≈ 2 TeV (this value is only reached in gauginomediated simplified models [87]). Recent results include a search in two-opposite-sign, same-flavor dilepton final state events [88] targeting squarks decaying through the next-to-lightest neutralino via a slepton or a Z boson and exclude masses up to ≈ 1550 GeV for a massless neutralino. Squarks decaying via charginos and next-to-lightest neutralinos in long decay chains including W and Z bosons are constrained with searches for same-sign dilepton or three-lepton final state events [89]: in this case, masses up to ≈ 1.7 TeV are excluded.

For single light squarks ATLAS also reports results of a dedicated search for pair production of scalar partners of charm quarks [90,91]. Assuming that the scalar-charm state exclusively decays into a charm quark and a neutralino, scalar-charm masses up to 900 GeV are excluded for neutralino masses below 260 GeV.

A summary of the most important squark and gluino mass limits for different interpretation approaches assuming R-parity conservation is shown in Table 88.1. For gluino masses rather similar limits of about 2.3–2.4 TeV are obtained from different model assumptions, indicating that the LHC is indeed probing direct gluino production at the TeV scale and beyond. However, for neutralino masses above approximately 1.2 to 1.6 TeV, even in the best case scenarios, ATLAS and CMS searches do not place any limits on the gluino mass. Limits on direct squark production, on the other hand, depend strongly on the chosen model. For neutralino masses above ≈ 600 GeV no limits on any direct squark pair production scenario are placed by the LHC.

Table 88.1: Summary of squark mass and gluino mass limits using different interpretation approaches assuming *R*-parity conservation. Masses in this table are provided in GeV. Further details about the assumptions and analyses from which these limits are obtained are discussed in the corresponding sections of the text.

Model	Assumption	$m_{ ilde{q}}$	$m_{\tilde{g}}$
Simplified models $\tilde{g}\tilde{g}$			
$\tilde{g} \to q \bar{q} \tilde{\chi}_1^0$	$m_{\tilde{\chi}_1^0} = 0$	-	≈ 2300
	$m_{\tilde{\chi}_1^0} > \approx 1200$	-	no limit
$\tilde{g} \to b \bar{b} \tilde{\chi}_1^0$	$m_{\tilde{\chi}_{1}^{0}} = 0$	-	≈ 2440
	$m_{\tilde{\chi}_1^0} > \approx 1600$	-	no limit
$\tilde{g} \to t\bar{t}\tilde{\chi}_1^0$	$m_{\tilde{\chi}_{1}^{0}} = 0$	-	≈ 2400
	$m_{\tilde{\chi}_1^0} > \approx 1400$	-	no limit
Simplified models $\tilde{q}\tilde{q}$			
$\tilde{q} o q \tilde{\chi}_1^0$	$m_{\tilde{\chi}_1^0} = 0$	≈ 1900	_
	$m_{\tilde{\chi}_1^0} > \approx 800$	no limit	_
$\tilde{u}_L \to q \tilde{\chi}_1^0$	$m_{\tilde{\chi}_1^0} = 0$	≈ 1300	-
	$m_{\tilde{\chi}_1^0} > \approx 600$	no limit	_

88.6 Exclusion limits on bottom and top squarks masses in RPC scenarios

Besides placing stringent limits on first and second generation squark masses, the LHC experiments also search for the production of third generation squarks. SUSY at the TeV-scale is often motivated by naturalness arguments, most notably as a solution to cancel quadratic divergences in radiative corrections to the Higgs boson mass. In this context, the most relevant terms for SUSY phenomenology arise from the interplay between the masses of the third generation squarks and the Yukawa coupling of the top quark to the Higgs boson. This motivates a potential constraint on the masses of the top squarks and the left-handed bottom squark. Due to the large top quark mass, significant mixing between \tilde{t}_L and \tilde{t}_R is expected, leading to a lighter mass state \tilde{t}_1 and a heavier mass state \tilde{t}_2 . In the MSSM, the lightest top squark (\tilde{t}_1) can be the lightest squark.

Bottom squarks are expected to decay predominantly to $b\tilde{\chi}_1^0$ giving rise to the characteristic multi b-jet and $E_{\rm T}^{\rm miss}$ signature. Direct production of bottom squark pairs has been searched for at the Tevatron and at the LHC. Limits from the Tevatron are $m_{\tilde{b}} > 247$ GeV for a massless neutralino [92,93]. ATLAS has set a lower limit of $m_{\tilde{b}} > 1250$ GeV for massless neutralinos in this model [94] exploiting the two b-jets and missing transverse momentum analysis. For $m_{\tilde{\chi}_1^0} \approx 800$ GeV or higher no limit can be placed on direct bottom squark pair production in this simplified model. Limits from CMS are comparable [84]. Reinterpretations of the monojet analysis results can be used to constrain very compressed scenarios, with exclusion of masses up to 550 GeV in case of $\Delta m = m_{\tilde{b}} - m_{\tilde{\chi}_1^0} \approx 5$ GeV [86]. Further bottom squark decay modes have also been searched for by ATLAS [95–97] and CMS [76,98,99], for instance targeting more complex decay chains that include Higgs bosons in the cascade.

The top squark decay modes depend on the SUSY mass spectrum, and on the $\tilde{t}_{\rm L}$ - $\tilde{t}_{\rm R}$ mixture of the top squark mass eigenstate. If kinematically allowed, the two-body decays $\tilde{t} \to t \tilde{\chi}_1^0$ (which requires $m_{\tilde{t}} - m_{\tilde{\chi}_1^0} > m_t$) and $\tilde{t} \to b \tilde{\chi}^{\pm}$ (which requires $m_{\tilde{t}} - m_{\tilde{\chi}^{\pm}} > m_b$) are expected to dominate, depending on L-R mixture. If not, the top squark decay may proceed either via the two-body decay

 $\tilde{t} \to c\tilde{\chi}_1^0$ or through $\tilde{t} \to bf\bar{f}'\tilde{\chi}_1^0$ (where f and \bar{f}' denote a fermion-antifermion pair with appropriate quantum numbers). For $m_{\tilde{t}} - m_{\tilde{\chi}_1^0} > m_b$ the latter decay chain represents a four-body decay with a W boson, charged Higgs H^{\pm} , slepton $\tilde{\ell}$, or light flavor squark \tilde{q} , exchange. If the exchanged W boson and/or sleptons are kinematically allowed to be on-shell, the three-body decays $\tilde{t} \to Wb\tilde{\chi}_1^0$ and/or $\tilde{t} \to b\nu\tilde{\ell}(\tilde{\nu}\ell)$ will become dominant. For further discussion on top squark decays see for example Ref. [100].

Limits from LEP on the \tilde{t}_1 mass are $m_{\tilde{t}} > 96$ GeV in the charm plus neutralino final state, and > 93 GeV in the lepton, b-quark and sneutrino final state [72].

The Tevatron experiments have performed a number of searches for top squarks, often assuming direct pair production. In the $b\ell\tilde{\nu}$ decay channel, and assuming a 100% branching fraction, limits are set as $m_{\tilde{t}} > 210$ GeV for $m_{\tilde{\nu}} < 110$ GeV and $m_{\tilde{t}} - m_{\tilde{\nu}} > 30$ GeV, or $m_{\tilde{t}} > 235$ GeV for $m_{\tilde{\nu}} < 50$ GeV [101, 102]. In the $\tilde{t} \to c\tilde{\chi}_1^0$ decay mode, a top squark with a mass below 180 GeV is excluded for a neutralino lighter than 95 GeV [103, 104]. In both analyses, no limits on the top squark can be set for heavy sneutrinos or neutralinos. In the $\tilde{t} \to b\tilde{\chi}_1^\pm$ decay channel, searches for a relatively light top squark have been performed in the dilepton final state [105, 106]. The CDF experiment sets limits in the $\tilde{t} - \tilde{\chi}_1^0$ mass plane for various branching fractions of the chargino decay to leptons and for two values of $m_{\tilde{\chi}_1^\pm}$. For $m_{\tilde{\chi}_1^\pm} = 105.8$ GeV and $m_{\tilde{\chi}_1^0} = 47.6$ GeV, top squarks between 128 and 135 GeV are excluded for W-like leptonic branching fractions of the chargino.

The LHC experiments have improved these limits substantially and developed dedicated searches for all potential top-squark decay modes. This is well depicted in Fig. 88.6, where a summary of the limits on the top squark mass are reported for the single decay chain of $\tilde{t} \to t \tilde{\chi}^0_1$ as well as for the three-body and four-body decay modes. Interpretations are carried out in simplified models hence care must be taken when interpreting these limits in the context of more complete SUSY models.

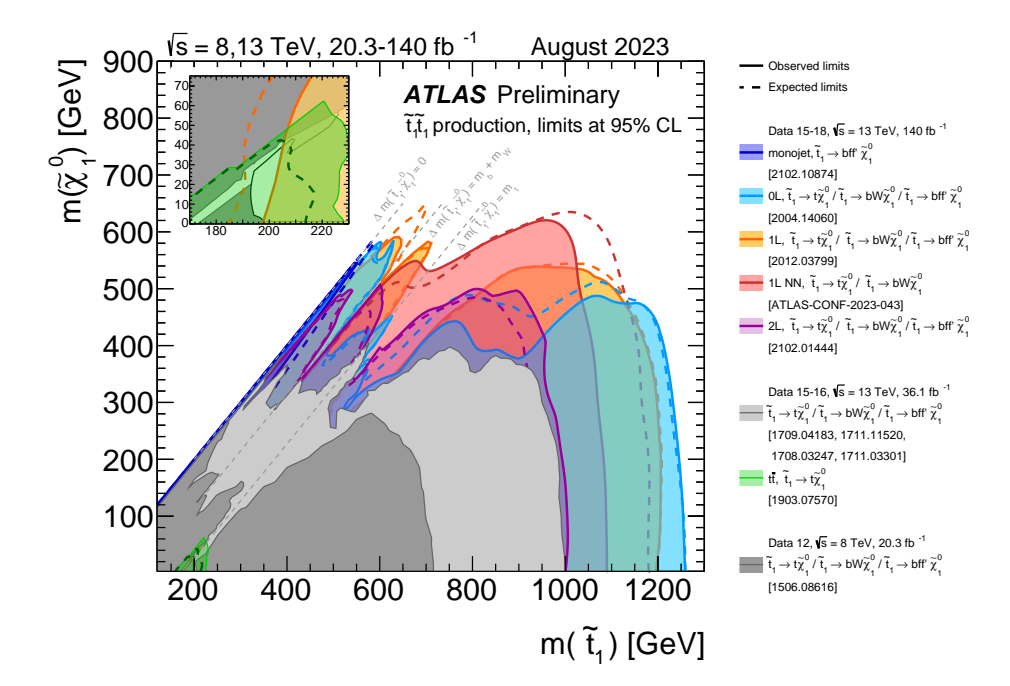


Figure 88.6: A summary of the 95% C.L. exclusion contours in the stop-neutralino mass plane for various possible decay chains, including two-, three- and four-body decays, as obtained in dedicated analyses by ATLAS.

The most important searches for the top squark decay topology are dedicated searches requiring zero or one isolated lepton, modest $E_{\rm T}^{\rm miss}$, and four or more jets out of which at least one jet must be reconstructed as a b-jet [51,76,84,85,107–109]. For example, using an all-hadronic analysis, CMS excludes top squarks with masses below about 1300 GeV in this model for light neutralinos, while for $m_{\tilde{\chi}_1^0} > 700$ GeV no limits can be provided [85]. Equivalent constraints are set by the ATLAS all-hadronic search [107]. Analyses targeting final state events characterised by the presence of one lepton (electron or muon) have similar albeit lower sensitivity in the $\tilde{t} \to t \tilde{\chi}_1^0$ decay mode, see for instance the recent ATLAS result [109] using NN methods.

Single and di-lepton analyses are most sensitive to models where the top squark decay exclusively proceeds via the chargino mediated decay chain $\tilde{t} \to b \tilde{\chi}_1^\pm$, $\tilde{\chi}_1^\pm \to W^{\pm(*)} \tilde{\chi}_1^0$. In this case, top squark mass exclusion limits vary strongly with the assumptions made on the $\tilde{t}-\tilde{\chi}_1^\pm-\tilde{\chi}_1^0$ mass hierarchy. For example, for $m_{\tilde{\chi}_1^\pm}=(m_{\tilde{t}}+m_{\tilde{\chi}_1^0})/2$, a stop mass below ≈ 1150 GeV for a light $\tilde{\chi}_1^0$ is excluded by CMS, while no limit can be placed for $m_{\tilde{\chi}_1^0}>550$ GeV [51]. These limits, however, can weaken significantly when other assumptions about the mass hierarchy or the decay of the charginos are imposed [51,110–112].

Other analyses with zero, one or two leptons target this kinematic region [113–119], also providing sensitivity in the case of alternative decay modes of the top squark, *i.e.* including tau sleptons [112,120–122] or Higgs and Z bosons in the decay chain [123].

If the decays $\tilde{t} \to t \tilde{\chi}_1^0$ and $\tilde{t} \to b \tilde{\chi}_1^{\pm}$, $\tilde{\chi}_1^{\pm} \to W^{\pm(*)} \tilde{\chi}_1^0$ are kinematically forbidden, the decay chains $\tilde{t} \to Wb \tilde{\chi}_1^0$ and $\tilde{t} \to c \tilde{\chi}_1^0$ can become important. The one-lepton ATLAS search [108] provides for the kinematic region $m_{\tilde{t}} - m_{\tilde{\chi}^{\pm}} > m_b + m_W$ lower limits on the top squark mass of ≈ 700 GeV for a neutralino lighter than ≈ 570 GeV, as also shown in Fig. 88.6. For the kinematic region in which even the production of real W bosons is not allowed, ATLAS and CMS improve the Tevatron limit on $\tilde{t} \to c \tilde{\chi}_1^0$ substantially. Based on a monojet analysis [86] ATLAS excludes top squark masses below $m_{\tilde{\chi}_1^0} \approx 550$ GeV along the kinematic boundary for the $\tilde{t} \to c \tilde{\chi}_1^0$ decay. The ATLAS monojet analysis also places similar boundaries for the other decay chain relevant in this phase region, $\tilde{t} \to bf \bar{f}' \tilde{\chi}_1^0$. Other analyses, such as the search in events with one leptons and jets, are also sensitive to this decay mode: the ATLAS one-lepton analysis excludes up to ≈ 650 GeV for $\Delta m = m_{\tilde{t}}, m_{\tilde{\chi}_1^0} \approx 50$ GeV [108]. A recent dedicated analysis for $\tilde{t} \to c \tilde{\chi}_1^0$ exploiting c-tagging excludes stop masses below about 900 GeV for $m_{\tilde{\chi}_1^0}$ below 420 GeV [91]. Also a topology where one stop decays through $\tilde{t} \to c \tilde{\chi}_1^0$ and the other one through $\tilde{t} \to t \tilde{\chi}_1^0$ has been considered [91, 124] and limits have been placed, in the case of equal branching ratios, 800 GeV for light neutralinos and 600 GeV in the compressed region.

The CMS collaboration uses the hadronic searches [85, 114, 116] to place constraints on stop decay into charm-quark and excludes $m_{\tilde{t}} \approx 630$ GeV for $\Delta m = m_{\tilde{t}}, m_{\tilde{\chi}_1^0} \approx 50$ GeV [85]. Constraints are also set in case of $\tilde{t} \to bf\bar{f}'\tilde{\chi}_1^0$, with CMS excluding masses up to 480 and 700 GeV for $\Delta m = m_{\tilde{t}}, m_{\tilde{\chi}_1^0} \approx 10$ and 80 GeV, respectively [125].

In general, the variety of top squark decay chains in the phase space region where $\tilde{t} \to t \tilde{\chi}_1^0$ is kinematically forbidden represents a challenge for the experimental search program but more data and refined analyses in Run 2 have further improved the sensitivity in this difficult but important region of SUSY parameter space, and more is expected for future Runs of the LHC. Precision SM measurements can also provide important insights to such challenging regions. For instance, analyses of $t\bar{t}$ spin correlations can be used to set constraints on top squark masses close to the top-quark mass. ATLAS [126] excludes the mass region between 150 and 230 GeV for kinematically allowed values of the neutralino mass. CMS [119] results cover a similar mass range.

Table 88.2: Summary of bottom and top squark mass limits using different interpretation approaches assuming *R*-parity conservation. Masses in this table are provided in GeV. Further details about the assumptions and analyses from which these limits are obtained are discussed in the corresponding sections of the text.

Model	Assumption	$m_{ ilde{q}}$
$ ilde{b} ightarrow b ilde{\chi}_1^0$	$m_{\tilde{\chi}_{1}^{0}} = 0$	≈ 1250
	$m_{\tilde{\chi}_1^0} > \approx 700$	no limit
$ ilde{t} ightarrow t ilde{\chi}_1^0$	$m_{\tilde{\chi}_{1}^{0}} = 0$	≈ 1300
	$m_{\tilde{\chi}_1^0} > \approx 600$	no limit
$\tilde{t} \to b \tilde{\chi}_1^{\pm}$	$m_{\tilde{\chi}_{1}^{0}} = 0$	≈ 1150
$(m_{\tilde{\chi}_1^{\pm}} = (m_{\tilde{t}} - m_{\tilde{\chi}_1^0})/2)$	$m_{\tilde{\chi}_1^0} > \approx 550$	no limit
$\tilde{t} \to W b \tilde{\chi}_1^0$	$m_{\tilde{\chi}_1^0} \ll 570$	≈ 700
$\underline{(m_W < m_{\tilde{t}} - m_{\tilde{\chi}^0} < m_t)}$	-	
$\tilde{t} \to c \tilde{\chi}_1^0$	$m_{\tilde{t}} - m_{\tilde{\chi}_1^0} \approx 50$	≈ 900
	$m_{ ilde{t}}pprox m_{ ilde{\chi}_1^0}$	≈ 550
$\tilde{t} \to bff'\tilde{\chi}^0_1$	$m_{\tilde{t}} - m_{\tilde{\chi}_1^0} \approx 50$	≈ 650
$\underline{\qquad (m_{\tilde{t}} - m_{\tilde{\chi}^0} < m_W)}$	$m_{ ilde{t}} pprox m_{ ilde{\chi}_1^0}$	≈ 550

88.7 Exclusion limits on the masses of charginos, neutralinos and sleptons in RPC scenarios

Charginos, neutralinos and sleptons are produced through electroweak interactions and their cross sections depend on the assumptions made for mass and mixing parameters.

Charginos and neutralinos carry no color charge and the mixing of the charged wino and higgsino states (for charginos), and the neutral bino, wino and higgsino states (for neutralinos), is determined by a limited number of parameters. For charginos these are the wino mass parameter M_2 , the higgsino mass parameter μ , and $\tan \beta$, and for neutralinos these are the same parameters plus the bino mass parameter M_1 . If one of the parameters M_1 , M_2 or μ is substantially smaller than the others, the chargino/neutralino composition would be dominated by specific states, which are referred to as bino-like ($M_1 \ll M_2, \mu$), wino-like ($M_2 \ll M_1, \mu$), or higgsino-like ($\mu \ll M_1, M_2$). If gaugino mass unification at the GUT scale is assumed, a relation between M_1 and M_2 at the electroweak scale follows: $M_1 = 5/3 \tan^2 \theta_W M_2 \approx 0.5 M_2$, with θ_W the weak mixing angle. At hadron colliders the largest production rates arise when the lightest chargino and the next-to-lightest neutralino are wino-like and nearly mass-degenerate, forming an SU(2) triplet. In this case the LSP is typically bino-like. If instead the higgsino mass parameter is much smaller than the gaugino masses, the two lightest neutralinos and the lightest chargino form an approximately mass-degenerate SU(2) doublet; production rates are lower and the mass spectrum is compressed.

In models with slepton and gaugino mass unification at the GUT scale, the superpartner of the right-handed lepton, $\tilde{\ell}_R$, is expected to be lighter than the left-handed one, $\tilde{\ell}_L$. Cross sections depend on the L-R mixing which in turn depends on the mass of the fermion and other parameters. For tau sleptons there may be considerable mixing between the L and R states, leading to a significant mass difference between the lighter $\tilde{\tau}_1$ and the heavier $\tilde{\tau}_2$.

Fig. 88.7 [127,128] (see also Ref. [73] for further details) shows typical production cross sections at hadron colliders for electroweakinos under various assumptions and considering a center-of-mass

energy of 13 TeV. For masses of several hundreds of GeV, they are at least two orders of magnitude smaller than for colored SUSY particles. Thanks to the large data samples collected at the LHC, the sensitivity of LEP and Tevatron searches for direct chargino/neutralino or slepton production has been surpassed in several regions of SUSY parameter space.

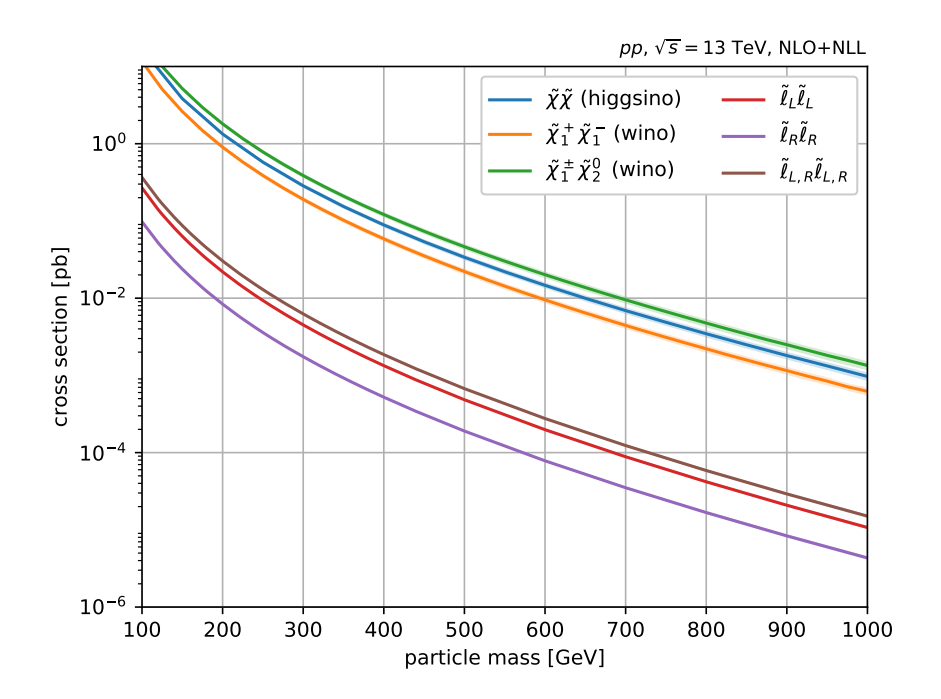


Figure 88.7: Cross sections for pair production of charginos, neutralinos and sleptons calculated for 13 TeV centre-of-mass energy at NLO plus next-to-leading-log (NLL) precision. Wino-like $\tilde{\chi}_1^{\pm}\tilde{\chi}_2^0$ and $\tilde{\chi}_1^{+}\tilde{\chi}_1^{-}$ productions are calculated in a limit of mass-degenerate $\tilde{\chi}_1^{\pm}$ and $\tilde{\chi}_2^0$, light bino $\tilde{\chi}_1^0$, and with all the other sparticles assumed to be heavy and decoupled. Higgsino-like cross sections assume mass-degenerate $\tilde{\chi}_1^{\pm}$, $\tilde{\chi}_2^0$ and $\tilde{\chi}_1^0$. For slepton pair cross sections, left(right)-handed only or 50% mixed states are considered.

88.7.1 Exclusion limits on chargino masses

The lightest chargino $\tilde{\chi}_1^{\pm}$ is searched for either considering pair production, or through associated production of $\tilde{\chi}_1^{\pm}$ and the next-to-lightest neutralino, $\tilde{\chi}_2^0$, if they are assumed to be degenerate in mass. If kinematically allowed, two body decay modes such as $\tilde{\chi}^{\pm} \to \tilde{f} \bar{f}'$ (including $\ell \tilde{\nu}$ and $\tilde{\ell} \nu$) are dominant. If not, three-body decays $\tilde{\chi}^{\pm} \to f \bar{f}' \tilde{\chi}_1^0$, mediated through virtual W bosons or sfermions, become dominant. If sfermions are heavy, the W mediation dominates, and $f \bar{f}'$ are distributed with branching fractions similar to W decay products (barring phase space effects for small mass gaps between $\tilde{\chi}^{\pm}$ and $\tilde{\chi}^0$). If, on the other hand, sleptons are light enough to play a significant role in the decay, leptonic final states will be enhanced.

At LEP, $\tilde{\chi}_1^+ \tilde{\chi}_1^-$ is the dominant production process. Charginos have been searched for in fully-hadronic, semi-leptonic and fully leptonic decay modes [129, 130]. A general lower limit on the lightest chargino mass of 103.5 GeV is derived, except in corners of phase space with low electron sneutrino mass, where destructive interference in chargino production, or two-body decay modes, play a role. The limit is also affected if the mass difference between $\tilde{\chi}_1^{\pm}$ and $\tilde{\chi}_1^0$ is small; dedicated searches for such scenarios set a lower limit of 92 GeV.

At the Tevatron, charginos have been searched for via associated production of $\tilde{\chi}_1^{\pm} \tilde{\chi}_2^0$ [131,132]. Decay modes involving multilepton final states provide the best discrimination against the large multijet background. Analyses have looked for at least three charged isolated leptons, for two leptons with missing transverse momentum, or for two leptons with the same charge. Depending on the $(\tilde{\chi}_1^{\pm} - \tilde{\chi}_1^0)$ and/or $(\tilde{\chi}_2^0 - \tilde{\chi}_1^0)$ mass differences, leptons may have soft transverse momentum.

At the LHC, the search strategy is similar to that at the Tevatron but it also exploits the large datasets collected to target missing momentum and fully-hadronic final states and consider $\tilde{\chi}_1^+ \tilde{\chi}_1^-$ production only i.e. releasing the assumption of $\tilde{\chi}_1^\pm, \tilde{\chi}_2^0$ mass degeneracy. Furthermore, compressed SUSY spectra are searched for considering low-momentum leptons recoiling against an ISR jet.

Chargino pair production is mainly searched for in the dilepton plus missing momentum final state. In a simplified model interpretation of the results where only the $\tilde{\chi}_1^+ \tilde{\chi}_1^-$ process is considered and assuming mediation of the chargino decay by light sleptons (\tilde{e} and $\tilde{\mu}$), ATLAS [133] and CMS [134] set limits on the chargino mass up to 1 TeV for massless LSPs, but no limits on the chargino mass can be set for $\tilde{\chi}_1^0$ heavier than 480 GeV. Limits are fairly robust against variation of the slepton mass, unless the mass gap between sparticles becomes small enough that the charged lepton has a too low-momentum to be reconstructed. For decays mediated through $\tilde{\tau}$ or $\tilde{\nu}_{\tau}$, recent results reach limits of 970 GeV as set by ATLAS [135] for LSPs not heavier than 440 GeV. The CMS experiment provides limits using Run 2 data [136].

In case slepton masses are higher than the mass of the chargino, searches are performed for charginos decaying via a W boson. Constraints on pair-produced pure-wino charginos using various decay channels have been recently summarized by ATLAS using statistical combinations of Run 2 searches [137]. The combination of the search results closes the gaps left by the individual searches in this simplified model, with chargino masses excluded up to 800 GeV for massless neutralinos. No limits are set for LSP masses above 170 GeV. Individual channels include 2-lepton final state events [133], resulting in masses below 420 GeV being excluded for massless LSPs. In the challenging case where the difference between chargino and LSP masses is close to that of the W boson, dedicated searches have been carried out by ATLAS [138], excluding chargino masses up to 140 GeV. Searches have also been carried out in the single lepton final state. ATLAS excludes chargino masses between 260 and 520 GeV for a massless LSP [139]. Further extension of the sensitivity in the high-mass region is achieved by ATLAS [140] and CMS [141] exploiting the large branching ratio of fully-hadronic final states and the identification of boosted W bosons through large-radius jets and jet substructure information. Considering only wino-like chargino pair production in case of a massless LSP, ATLAS excludes a region between 630 GeV and 760 GeV, while CMS excludes between 290 GeV and 670 GeV. No limits are set for LSP masses above 200 GeV.

Several final states characterized by the presence of missing transverse momentum are studied to set limits on the chargino mass through $\tilde{\chi}_1^{\pm}\tilde{\chi}_2^0$ associated production. Usually, wino-like $\tilde{\chi}_1^{\pm}$ and $\tilde{\chi}_2^0$ and bino-like $\tilde{\chi}_1^0$ are assumed with $m_{\tilde{\chi}_1^{\pm}} = m_{\tilde{\chi}_2^0}$, leaving $m_{\tilde{\chi}_1^{\pm}}$ and $m_{\tilde{\chi}_1^0}$ free. Higgsino models with small mass differences among the electroweakinos are targeted using low-momentum lepton signatures. Again, the branching fraction of leptonic final states is determined by the slepton masses. If the decay is predominantly mediated by a light $\tilde{\ell}_L$, i.e. $\tilde{\ell}_R$ is assumed to be heavy, the three charged-lepton flavors will be produced in equal amounts, and a multi-lepton signature is favored. For simplicity, $\tilde{\ell}_L$ and $\tilde{\nu}$ are taken to be nearly mass-degenerate, and diagrams with sneutrinos are included.

In such a scenario, ATLAS [142] and CMS [143] exclude chargino masses below 1450 GeV for massless LSPs; no limits are set for LSP masses above 1 TeV. If the decay is dominated by a light

 $\tilde{\ell}_{\rm R}$, the chargino cannot be a pure wino but needs to have a large higgsino component, preferring the decays to tau leptons. Limits are set in various scenarios. If, like for $\tilde{\ell}_{\rm L}$, a flavor-democratic scenario is assumed (τ -enriched scenario), CMS sets limits of 1150 GeV on the chargino mass for massless LSPs, but under the assumption that both $\tilde{\chi}_1^{\pm}$ and $\tilde{\chi}_2^0$ decay leads to tau leptons in the final state (τ -dominated scenario), the chargino mass limit deteriorates to 970 GeV for massless LSPs [143]. ATLAS assumes a simplified model in which staus are significantly lighter than the other sleptons and search for a similar multi-tau final state, setting a lower limit on the chargino mass of 1160 GeV in this model [135].

If sleptons are heavy, the chargino is assumed to decay to a W boson plus LSP, and the $\tilde{\chi}_2^0$ into Z plus LSP (WZ searches) or H plus LSP (WH searches). Searches for the WZ channel exploit events with either two same-sign leptons or three leptons, a single lepton, or with no leptons (all-hadronic). If $\tilde{\chi}_2^0$ decays through a Higgs boson with $m_H = 125$ GeV, search strategies depend on the SM-like Higgs decay modes and branching fractions. Higgs bosons in the final state are identified by either two jets originating from bottom quarks $(h \to b\bar{b})$, two photons $(h \to \gamma\gamma)$, or leptons from the WW, ZZ or $\tau\tau$ decay modes. Interpretations are also provided in scenarios where the $\tilde{\chi}_2^0$ does not decay exclusively into a Z or H boson and the LSP.

A combination of the results of several searches for the electroweak production of the supersymmetric partners of standard model bosons has been published by CMS [144]. In the case of wino-like $\tilde{\chi}_1^{\pm}\tilde{\chi}_2^0$ production, the combined CMS result gives an observed (expected) limit on the chargino mass of about 875 (950) GeV for the WZ topology. Limits on a higgsino-bino model where charginos decay to a W boson and the LSP up to 800 GeV are set in simplified models where it is degenerate with $\tilde{\chi}_2^0$ and $\tilde{\chi}_3^0$.

The recent ATLAS statistical combinations of Run 2 searches [137] excludes $\tilde{\chi}_1^{\pm}$ masses up to 1000 GeV, with no mass limits possible for LSP masses above 400 GeV. Searches for $\tilde{\chi}_1^{\pm}\tilde{\chi}_2^0$ production in events with three leptons and missing momentum allows to exclude wino-like chargino masses below 640 GeV for massless LSPs [145]. Results have also been reported for searches including same-sign lepton signal regions [146] and single lepton searches [139]. Limits are reduced in case of higgsino-like scenarios, with exclusion down to 210 GeV.

Additional constraints on the chargino mass are placed exploiting all-hadronic analyses. A wino-like (higgsino-like) chargino with mass up to 1060 (900) GeV is excluded by ATLAS [140] when the LSP mass is below 400 (240) GeV and the mass splitting is larger than 400 (450) GeV. This is also included in the Run 2 combination study. CMS [141] excludes wino-like charginos with mass up to 970 GeV for massless LSP.

Searches exploiting the presence of b-jets are most sensitive in the high-mass chargino region if $\tilde{\chi}_2^0$ decays through a Higgs boson, while analyses targeting photon pair or leptonic decays provide the best sensitivity in the region of low masses. CMS [147] sets lower limits on the chargino mass up to 820 GeV for massless LSPs, but vanish for LSP masses above 350 GeV using events with at least one lepton and missing transverse momentum in the final state. In the case of wino-like $\tilde{\chi}_1^{\pm}\tilde{\chi}_2^0$ production, the combined CMS result [144] gives an observed (expected) limit on the chargino mass of about 990 (1075) GeV for the WH topology, and 875 (1000) GeV for a mixed topology with WZ. Similar sensitivities are achieved by the ATLAS analyses [148–150], combined in [137].

In both the wino region (a characteristic of anomaly-mediated SUSY breaking models) and the higgsino region of the MSSM, the mass splitting between $\tilde{\chi}_1^{\pm}$ and $\tilde{\chi}_1^0$ is small. The chargino decay products are very soft and may escape detection. These compressed spectra are hard to detect, and have triggered dedicated search strategies.

Studies from ATLAS [151] and CMS [152] for charginos and neutralinos in a compressed mass

spectrum use initial state radiation and two or three low-momentum (soft) leptons. For wino-like charginos, assuming degenerate $\tilde{\chi}_1^{\pm}$ and $\tilde{\chi}_2^0$, exclusion contours in the chargino-mass versus $\Delta m(\tilde{\chi}_1^{\pm} - \tilde{\chi}_1^0)$ plane are derived. As an example, such charginos are excluded by CMS (ATLAS) below 280 (240) GeV for $\Delta m(\tilde{\chi}_1^{\pm} - \tilde{\chi}_1^0) = 10$ GeV. Considering the higgsino model, the masses probed by CMS reach up to 215 GeV for a mass difference of 7.5 GeV and 150 GeV in the highly compressed region with a mass difference of 3 GeV.

Recent ATLAS results [153] using vector boson fusion signatures and missing transverse momentum were interpreted in simplified RPC models in which the LSP is a bino-like neutralino with a mass similar to that of the lightest chargino and second-to-lightest neutralino, both of which are wino-like. Lower limits at 95% confidence level on the masses of NLSPs were established between 117 and 120 GeV when the LSP is within 1 GeV in mass. CMS has also searched for chargino-pair production through vector-boson-fusion [154], also targeting compressed mass spectra. Assuming degenerate $\tilde{\chi}_1^{\pm}$ and $\tilde{\chi}_2^0$, charginos with a mass below 112 GeV are excluded for $\Delta m(\tilde{\chi}_1^{\pm} - \tilde{\chi}_1^0) = 1$ GeV. CMS has published further searches for such compressed spectra with a soft tau lepton [155]. A combination of several searches for the electroweak production of winos, binos, higgsinos, and sleptons has also been recently been presented by CMS [144].

88.7.2 Exclusion limits on neutralino masses

In a considerable part of the MSSM parameter space, and in particular when demanding that the LSP carries no electric or color charge, the lightest neutralino $\tilde{\chi}^0_1$ is the LSP. If R-parity is conserved, such a $\tilde{\chi}^0_1$ is stable. Since it is weakly interacting, it will typically escape detectors unseen. Limits on the invisible width of the Z boson apply to neutralinos with a mass below 45.5 GeV, but depend on the Z-neutralino coupling. Such a coupling could be small or even absent; in such a scenario there is no general lower limit on the mass of the lightest neutralino [156]. In models with gaugino mass unification and sfermion mass unification at the GUT scale, a lower limit on the neutralino mass is derived from limits from direct searches, notably for charginos and sleptons, and amounts to 47 GeV [157]. Assuming a constrained model like the CMSSM, this limit increases to 50 GeV at LEP; however the strong constraints now set by the LHC increase such CMSSM-derived $\tilde{\chi}^0_1$ mass limits to well above a few hundred GeV (the latest reinterpretation only uses Run 1 data and indicates 200 GeV [158–160]).

In gauge-mediated SUSY breaking models (GMSB), the LSP is typically a gravitino, and the phenomenology is determined by the nature of the next-to-lightest supersymmetric particle (NLSP). A NLSP neutralino will decay to a gravitino and a SM particle whose nature is determined by the neutralino composition. Final states with two high $p_{\rm T}$ photons and missing momentum are searched for, and interpreted in gauge mediation models with bino-like neutralinos [161–167].

Assuming the production of at least two neutralinos per event, neutralinos with large non-bino components can also be searched for by their decay in final states with missing momentum plus any two bosons out of the collection γ, Z, H . A number of searches at the LHC have tried to cover the rich phenomenology predicted by the general gauge mediation model (GGM) where $\tilde{\chi}_1^0$ might decay with various BR in the Z and H decay modes [98,149,164,168–178]. As an example, strong constraints for decay modes involving Z and H bosons arise from full-hadronic searches on higgsino-like scenarios: ATLAS [140] excludes higgsino production with decays into a massless gravitino LSP in a mass range between 450 (500) GeV and 940 (850) GeV assuming BR = 1 (0.5) for the Z plus gravitino decay mode. Assuming only H plus gravitino decays, CMS [179] excludes a higgsino mass range between 175 GeV and 1025 GeV. Assuming a mix of γ, Z, H decays, a CMS search [167] in the photonic final state excludes higgsinos up to 1.05 TeV.

Heavier neutralinos, in particular $\tilde{\chi}_2^0$, have been searched for in their decays to the lightest neutralino plus a γ , a Z boson or a Higgs boson. Limits on electroweak production of $\tilde{\chi}_2^0$ plus $\tilde{\chi}_1^{\pm}$

from all-hadronic, same-sign dilepton and trilepton analyses have been discussed in the section on charginos; the assumption of equal mass of $\tilde{\chi}_2^0$ and $\tilde{\chi}_1^{\pm}$ make the limits on chargino masses apply to $\tilde{\chi}_2^0$ as well. Multilepton analyses have also been used to set limits on $\tilde{\chi}_2^0 \tilde{\chi}_3^0$ production; assuming equal mass and decay through light sleptons, limits are set up to 680 GeV for massless LSPs [180]. Again, compressed spectra with small mass differences between the heavier neutralinos and the LSP form the most challenging region.

Of particular relevance are supersymmetric models characterised by pure wino or pure higgsino states, with small mass splittings between $\tilde{\chi}_1^{\pm}$ and $\tilde{\chi}_1^0$, $\Delta m \sim 160\,\mathrm{MeV}$ for winos and $\sim 350\,\mathrm{MeV}$ for higgsinos. In this case, the $\tilde{\chi}_1^0$ is a natural candidate for dark matter (thermal relic), with pure winos predicted as $m_{\chi} \simeq 2.8-3.1\,\mathrm{TeV}$ and pure higgsinos with thermal mass near 1.1 TeV. Winos feature a large annihilation cross section and predictions are currently in tension with reinterpretations of gamma-ray bounds. Higgsinos have lower annihilation rates and, under specific assumptions on the dark matter density, are constrained up to 270 GeV [181] (see also the Dark Matter Chapter in this review for references and further details).

In $\tilde{\chi}_2^0$ decays to $\tilde{\chi}_1^0$ and a lepton pair, the lepton pair invariant mass distribution may show a structure that can be used to measure the $\tilde{\chi}_2^0 - \tilde{\chi}_1^0$ mass difference in case of a signal [37]. This structure, however, can also be used in the search strategy itself, as demonstrated by ATLAS [182, 183] and CMS [98, 184].

Fig. 88.8 summarizes some of the most recent results from ATLAS and CMS for chargino pair or chargino and next-to-lightest neutralino pair productions comparing results obtained with various assumptions. The limits on weak gauginos in simplified models are also summarized in Table 88.3. Only results for promptly decaying charginos and neutralinos are included: limits from searches focusing on long-lived particle scenarios are reported in Section 88.9.

Interpretations of the search results outside simplified models, such as in the phenomenological MSSM (see [185–190] and, most recently, [191]), show that the simplified model limits can translate into accurate constraints but must also be interpreted with care. Electroweak gauginos in models that are compatible with the relic density of dark matter in the Universe, for example, have particularly tuned mixing parameters and mass spectra, which are not always captured by the simplified models used.

88.7.3 Exclusion limits on slepton masses

The most model-independent searches for selectrons, smuons and staus originate from the LEP experiments [192]. Smuon production only takes place via s-channel γ^*/Z exchange. Search results are often quoted for $\tilde{\mu}_R$, since it is typically lighter than $\tilde{\mu}_L$ and has a weaker coupling to the Z boson; limits are therefore conservative. Decays are expected to be dominated by $\tilde{\mu}_R \to \mu \tilde{\chi}_1^0$, leading to two non-back-to-back muons and missing momentum. Slepton mass limits are calculated in the MSSM under the assumption of gaugino mass unification at the GUT scale, and depend on the mass difference between the smuon and $\tilde{\chi}_1^0$. A $\tilde{\mu}_R$ with a mass below 94 GeV is excluded for $m_{\tilde{\mu}_R} - m_{\tilde{\chi}_1^0} > 10$ GeV. The selectron case is similar to the smuon case, except that an additional production mechanism is provided by t-channel neutralino exchange. The \tilde{e}_R lower mass limit is 100 GeV for $m_{\tilde{\chi}_1^0} < 85$ GeV. Due to the t-channel neutralino exchange, $\tilde{e}_R \tilde{e}_L$ pair production was possible at LEP, and a lower limit of 73 GeV was set on the selectron mass regardless of the neutralino mass by scanning over MSSM parameter space [193]. The potentially large mixing between $\tilde{\tau}_L$ and $\tilde{\tau}_R$ not only makes the $\tilde{\tau}_1$ light, but can also make its coupling to the Z boson small. LEP lower limits on the $\tilde{\tau}$ mass range between 87 and 93 GeV depending on the $\tilde{\chi}_1^0$ mass, for $m_{\tilde{\tau}} - m_{\tilde{\chi}_1^0} > 7$ GeV [192].

At the LHC, pair production of sleptons is not only heavily suppressed with respect to pair production of colored SUSY particles but the cross section is also almost two orders of magnitude

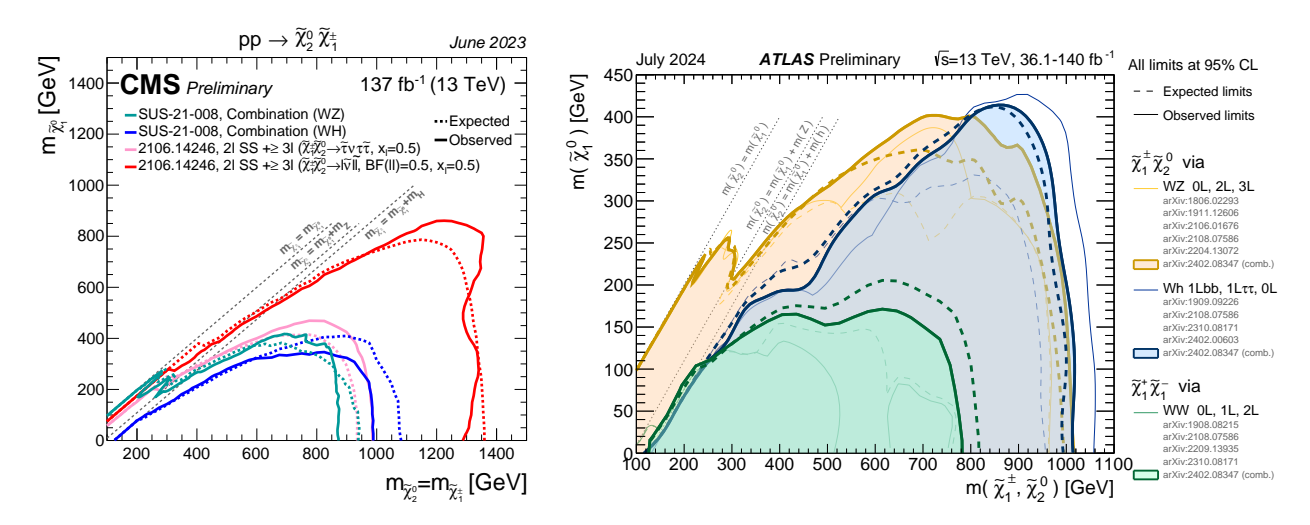


Figure 88.8: LHC exclusion limits on chargino and neutralino masses in a number of simplified models. Left: CMS limits on chargino and neutralino masses for pair production of charginos, pair production of heavier neutralinos, or pair production of chargino and neutralino, under a variety of assumptions including light sleptons mediating the decays. Right: ATLAS limits on chargino and neutralino masses for pair production of chargino and neutralino, under the assumption of decoupled sleptons, and chargino/neutralino decay through on- or off-shell W and Z or H.

smaller than the one of pair production of charginos and neutralinos. With the full data sets of Run 1 and Run 2, however, ATLAS and CMS have surpassed the sensitivity of the LEP analyses under certain assumptions.

ATLAS and CMS have searched for direct production of selectron pairs and smuon pairs at the LHC, with each slepton decaying to its corresponding SM partner lepton and the $\tilde{\chi}_1^0$ LSP. In simplified models, ATLAS [133] and CMS [184] set lower mass limits on sleptons of 700 GeV for degenerate $\tilde{\ell}_L$ and $\tilde{\ell}_R$, for a massless $\tilde{\chi}_1^0$ and assuming equal selectron and smuon masses, as shown in Fig. 88.9. The limits deteriorate with increasing $\tilde{\chi}_1^0$ mass due to decreasing missing momentum and lepton momentum. As a consequence, no limits are set for $\tilde{\chi}_1^0$ masses above 400 GeV. Limits are also derived without the assumption of slepton mass degeneracy [133,194].

A recent combination of the results of several searches for electroweakly produced supersymmetric particles has been published by CMS [144], with improved analysis techniques employed to optimize sensitivity for the compressed spectra in the slepton pair production models, providing constraints up to 210 GeV for mass splitting of 5 GeV between slepton and LSP.

Dedicated searches for sleptons with small mass difference between $\tilde{\ell}$ and $\tilde{\chi}_1^0$ are also performed by ATLAS [151, 195] demanding the presence of ISR jets. The most recent analysis includes an event selection optimization carried out depending on Δm and with ML techniques. Selectrons (smuons) with masses up to 300 (350) GeV are excluded for Δm between 2 GeV and 100 GeV on simplified models of selectron and smuon pair production. A dedicated search [138] in the challenging regime where the mass difference between the slepton and the LSP is close to the W mass results in exclusion of sleptons with masses up to 150 GeV for a mass-splitting between the sleptons and the LSP of 50 GeV.

ATLAS and CMS have also searched for $\tilde{\tau}$ -pair production. In simplified models, ATLAS excludes $\tilde{\tau}$ masses between 90 and 500 GeV assuming light $\tilde{\chi}^0_1$, combining the production of degenerate left- and right-handed $\tilde{\tau}$ s [135]. Purely left-handed $\tilde{\tau}$ s with masses up to 425 GeV and purely right-handed $\tilde{\tau}$ s with masses up to 350 GeV are also excluded. The CMS analysis [196] covers lower

Table 88.3: Summary of weak gaugino mass limits in simplified models, assuming R-parity conservation. Masses in the table are provided in GeV. Further details about assumptions and corresponding analyses are discussed in the text. Details on constraints for compressed scenarios from soft-lepton searches are not represented in the table.

Assumption	mass limit
$\tilde{\chi}_1^{\pm}$, all $\Delta m(\tilde{\chi}_1^{\pm}, \tilde{\chi}_1^0)$	> 92
$\tilde{\chi}_1^{\pm} \Delta m > 5, m_{\tilde{\nu}} > 300$	> 103.5
$\tilde{\chi}_{1}^{\pm}, m_{(\tilde{\ell}, \tilde{\nu})} = (m_{\tilde{\chi}_{1}^{\pm}} + m_{\tilde{\chi}_{1}^{0}})/2$	flavor-democratic
$m_{ ilde{\chi}_1^0} pprox 0$	> 1000
$ ilde{\chi}_1^{\pm}, m_{ ilde{\chi}_1^0}^{\gamma_1} > 480$	no LHC limit
$ ilde{\chi}_1^\pm,m_{(ilde{ ilde{ au}}, ilde{ u})}=(m_{ ilde{\chi}_1^\pm}+m_{ ilde{\chi}_1^0})/2$	$ ilde{ au} ext{-dominated}$
$m_{ ilde{\chi}_1^0}pprox 0$	> 970
$\tilde{\chi}_1^{\pm}, m_{\tilde{\chi}_1^0} > 440$	no LHC limit
$\frac{\tilde{\chi}_{1}^{\pm}, m_{\tilde{\ell}} > m_{\tilde{\chi}_{1}^{\pm}}}{\tilde{\chi}_{1}^{\pm}}$	
	> 420 and $290 - 760$
$m_{ ilde{\chi}_1^0}pprox 0 \ ilde{\chi}_1^\pm, m_{ ilde{\chi}_1^0}>120$	no LHC limit
$m_{\tilde{\chi}_1^{\pm}} = m_{\tilde{\chi}_2^0}, \ m_{\tilde{\ell}_L} = (m_{\tilde{\chi}_1^{\pm}} + m_{\tilde{\chi}_1^0})/2$	
$m_{\tilde{\chi}_1^0} pprox 0$	> 1450
$m_{\tilde{\chi}_1^0} > 1000$	no LHC limit
$\frac{m_{\tilde{\chi}_1^0} > 1000}{m_{\tilde{\chi}_1^{\pm}} = m_{\tilde{\chi}_2^0}, m_{\tilde{\ell}_{\rm R}} = (m_{\tilde{\chi}_1^{\pm}} + m_{\tilde{\chi}_1^0})/2}$	flavor-democratic
$m_{ ilde{\chi}_1^0}pprox 0$	> 1150
$m_{\tilde{\chi}_{1}^{0}} > 700$	no LHC limit
$m_{ ilde{\chi}_1^\pm} = m_{ ilde{\chi}_2^0}, m_{ ilde{ au}} = (m_{ ilde{\chi}_1^\pm} + m_{ ilde{\chi}_1^0})/2$	$\tilde{\tau}$ -dominated
$m_{ ilde{\chi}_1^0}pprox 0$	> 1160
$m_{\tilde{\chi}_1^0} > 450$	no LHC limit
$m_{\tilde{\chi}_{1}^{\pm}} = m_{\tilde{\chi}_{2}^{0}}, m_{\tilde{\ell}} > m_{\tilde{\chi}_{1}^{\pm}}, \text{BF}(WZ) = 1$	
$m_{ ilde{\chi}_1^0}pprox 0$	> 1000
$m_{\tilde{\chi}_1^0} > 400$	no LHC limit
$m_{\tilde{\chi}_1^{\pm}} = m_{\tilde{\chi}_2^0}, m_{\tilde{\ell}} > m_{\tilde{\chi}_1^{\pm}}, BF(WH) = 1$	
$m_{\tilde{\chi}_1^0} \approx 0$, wino-like $\tilde{\chi}_1^{\pm}$	> 1060
$m_{\tilde{\chi}_1^0} \approx 0$, higgsino-like $\tilde{\chi}_1^{\pm}$	> 900
$m_{\tilde{\chi}_1^0} > 400(240)$	no LHC limit wino(higgsino)-like
$m_{\tilde{\chi}_1^0}^{\lambda_1} > 300(270)$	indirect detection pure-wino(higgsino)

masses also closing the mass gap with LEP. In a search for hadronic final states, CMS [197] excludes purely left-handed $\tilde{\tau}$ s with masses between 115 and 340 GeV for massless LSP. The ATLAS search [135] for stau pair production in the fully hadronic final state excludes, for a massless LSP, degenerate left- and right-handed $\tilde{\tau}$ s with masses up to 480 GeV.

In gauge-mediated SUSY breaking models, sleptons can be (co-)NLSPs, *i.e.*, the next-to-lightest SUSY particles and almost degenerate in mass, decaying to a lepton and a gravitino. This decay

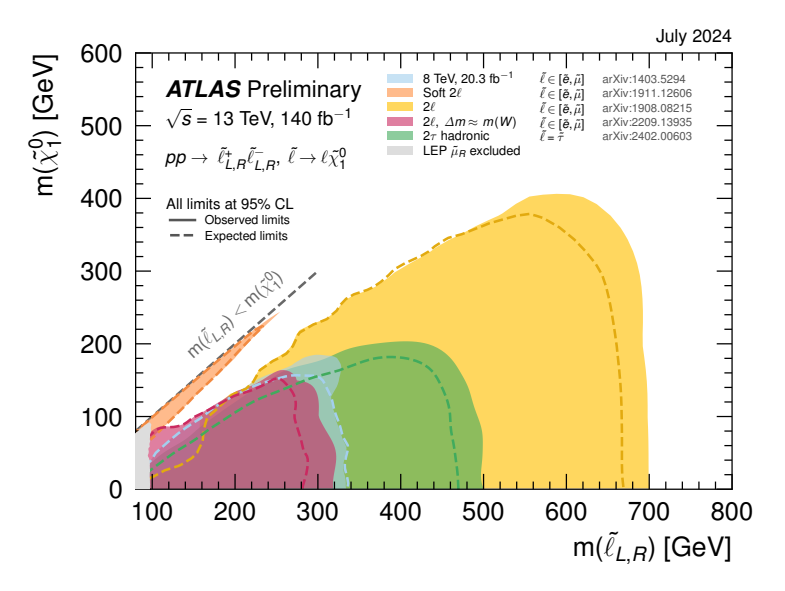


Figure 88.9: LHC exclusion limits on slepton (selectron, smuon and stau) masses, assuming equal masses of selectrons and smuons, degeneracy of $\tilde{\ell}_L$ and $\tilde{\ell}_R$, and a 100% branching fraction for $\tilde{\ell} \to \ell \tilde{\chi}_1^0$.

can either be prompt, or the slepton can have a non-zero lifetime. Combining several analyses, lower mass limits on $\tilde{\mu}_R$ of 96.3 GeV and on \tilde{e}_R of 66 GeV are set for all slepton lifetimes at LEP [198]. In a considerable part of parameter space in these constrained models, the $\tilde{\tau}$ is the NLSP. The LEP experiments have set lower limits on the mass of such a $\tilde{\tau}$ between 87 and 97 GeV, depending on the $\tilde{\tau}$ lifetime. ATLAS and CMS have searched for final states with τ s, jets and missing transverse momentum, and have interpreted the results in GMSB models setting limits

Table 88.4: Summary of slepton mass limits from LEP and LHC, assuming R-parity conservation and 100% branching fraction for $\tilde{\ell} \to \ell \tilde{\chi}_1^0$. Masses in this table are provided in GeV.

Assumption	$m_{ ilde{\ell}}$
$\tilde{\mu}_{\rm R}, \Delta m(\tilde{\mu}_{\rm R}, \tilde{\chi}_1^0) > 10$	> 94
$\tilde{e}_{\mathrm{R}}, \Delta m(\tilde{e}_{\mathrm{R}}, \tilde{\chi}_{1}^{0}) > 10$	> 94
\tilde{e}_{R} , any Δm	> 73
$\tilde{\tau}_{\mathrm{R}}, \Delta m(\tilde{\tau}_{\mathrm{R}}, \tilde{\chi}_1^0) > 7$	> 87
$\tilde{\nu}_e, \Delta m(\tilde{e}_{\mathrm{R}}, \tilde{\chi}_1^0) > 10$	> 94
$\overline{m_{\tilde{e}_{\rm L,R}} = m_{\tilde{\mu}_{\rm L,R}}, m_{\tilde{\chi}_1^0} \approx 0}$	> 700
$m_{\tilde{\chi}_1^0} > \approx 400$	no LHC limit
$m_{\tilde{ au}_{\rm L}} = m_{\tilde{ au}_{\rm R}}, m_{\tilde{\chi}_1^0} \approx 0$	> 500
$m_{\tilde{\chi}_1^0} > \approx 200$	no LHC limit
$m_{\tilde{ au}_{ m L}},m_{\tilde{\chi}_1^0}pprox 0$	> 425
$m_{\tilde{\chi}_1^0} > \approx 150$	no LHC limit
$m_{\tilde{ au}_{\mathrm{R}}}, m_{\tilde{\chi}_{1}^{0}} pprox 0$	> 350
$m_{\tilde{\chi}_1^0} > \approx 100$	no LHC limit

on the model parameters [199,200]. CMS has interpreted a multilepton analysis in terms of limits on gauge mediation models with slepton NLSP [201]. CDF has put limits on gauge mediation models at high $\tan \beta$ and slepton NLSP using an analysis searching for like-charge light leptons and taus [202].

The invisible width of the Z boson puts a lower limit on the sneutrino mass of about 45 GeV [203]. Tighter limits are derived from other searches, notably for gauginos and sleptons, under the assumption of gaugino and sfermion mass universality at the GUT scale, and amount to approximately 94 GeV in the MSSM [203].

The limits on sleptons in simplified models are summarized in Table 88.4.

88.8 Exclusion limits on promptly decaying sparticle masses in RPV scenarios

The large variety of possible configurations for non-zero λ , λ' and λ'' couplings in RPV SUSY scenarios leads to a huge number of potential signatures to be investigated in the strong and electroweak sectors. The lightest supersymmetric particle can be any particle, although most of the models considered at the LHC assume that to be the lightest neutralino, and can have a prompt or displaced decay. Cascade decays of sparticles down to the LSP can also be prompt or displaced depending on the strength of the couplings involved, although typically such cascades are dominated by gauge couplings which are prompt. In this section, we review dedicated searches for scenarios with small non-zero RPV couplings but still large enough to allow prompt decays of the sparticles involved (see Section 88.9 for examples of dedicated signatures searches for non-prompt decays).

Prompt RPV gluino and squark decays are searched for in final states generally characterised by the presence of multiple leptons or jets and moderate or no missing transverse momentum.

Searches in multilepton final states [89, 169, 204–208] set lower gluino mass limits between 1 and 2.5 TeV for decays mediated by λ and λ' couplings, with strong dependence on the couplings involved, the neutralino mass and the lepton flavor. Multijet final states have been used to search for fully hadronic gluino decays involving λ'' couplings, by CDF [209], ATLAS [96, 210–213] and CMS [214–216]. Lower gluino mass limits range between 600 and 2000 GeV depending on neutralino mass and flavor content of the final state. ATLAS [217] also searched in events characterised by high jet multiplicity, at least one isolated light lepton and either zero or at least three b-tagged jets, reaching as high as 2.4 TeV in gluino mass. If gluinos decay via top squarks into tbd final states through a non-zero λ''_{313} coupling, a search for same-sign/three-lepton events can be effective. ATLAS [89] sets a lower limit of 1.65 TeV for a top squark with a mass below 1.45 TeV.

RPV production of single squarks via a λ' -type coupling has been studied at HERA. In such models, a lower limit on the squark mass of the order of 275 GeV has been set for electromagnetic-strength-like couplings $\lambda' = 0.3$ [218]. At the LHC, prompt [205,208,219] R-parity violating squark decays have been searched for, with mass limits being very model-dependent.

Dedicated searches for RPV top squarks (at production and/or in decays) have been carried out in the past decades. Production of single top squarks has been searched for at LEP, HERA, and the Tevatron. For example, an analysis from the ZEUS collaboration [220] makes an interpretation of its search result assuming top squarks to be produced via a λ' coupling and decay either to $b\tilde{\chi}_1^{\pm}$ or R-parity-violating to a lepton and a jet. Limits are set on λ'_{131} as a function of the top squark mass in an MSSM framework with gaugino mass unification at the GUT scale. CMS and ATLAS have performed several searches for top squarks using a variety of multilepton and/or multijet final states and Run 2 data. The λ' -mediated top squark decay $\tilde{t} \to b\ell$ has been studied by ATLAS for prompt decays [221,222], and by ATLAS and CMS for non-prompt decays [223–225], setting limits up to 1.4 – 1.9 TeV in simplified models for this mode. CMS also searched for the λ' -mediated decay $\tilde{t} \to b\ell qq$, setting lower stop mass limits of 890 GeV (e) or 1000 GeV (μ) [226]. The fully hadronic R-parity violating top squark decays $\tilde{t} \to bs$, $\tilde{t} \to ds$, and $\tilde{t} \to bd$, involving λ'' , have been

searched for by ATLAS [96,205,211,227,228], and CMS [229,230]. Other recent searches target top squarks decaying through cascades into several b- and light-quarks, for example as in [231]. The most recent results set limits up to 1.35 TeV in top-squark mass [217] if decays include top- and b-quarks [217]. Constraints on masses up to 700 GeV are found if the top squarks decays include top- and light-quarks [232,233].

Various searches for multi-lepton and lepton plus jets events are interpreted in a model with RPV decays of charginos and neutralinos (including the LSP) involving a non-zero λ [169, 204, 208] or λ' [205, 213, 234, 235] coupling. Neutralino decays involving non-zero λ'' lead to fully hadronic final states, and searches for multi-jet events and jet-pair resonances are used to set limits, typically on the production of colored particles like top squarks or gluinos, which are assumed to be the primary produced sparticles in these interpretations, as discussed earlier. For instance, the ATLAS search [217] in events with one lepton and high jet multiplicity excludes up to 320 (365) GeV in higgsino (wino) masses. If top quarks arise in the decay of the neutralino, lepton-enriched final state events are also relevant, see for example the results in [146]. The multilepton search in [236] set limits on the production of charginos and neutralinos for a minimal SUSY model with an approximate B-L symmetry. In this case, charginos and neutralinos with masses between 100 GeV and 1.1 TeV are excluded depending on the assumed decay BR into a lepton plus a W, Z or H boson. Finally, recent results from ATLAS [146] set the first experimental constraints on bilinear RPV models (bRPV) with degenerate higgsino masses exploiting same-sign/three-lepton signatures, excluding masses smaller than 440 GeV.

Limits also exist on sleptons in RPV models, both from LEP and the Tevatron experiments. From LEP, lower limits on $\tilde{\mu}_R$ and \tilde{e}_R masses in such models are 97 GeV, and the limits on the stau mass are very close: 96 GeV [237]. CMS has searched for resonant smuon production in a modified CMSSM scenario [238], putting limits on λ'_{211} as a function of $m_0, m_{1/2}$. Production of pairs of sneutrinos in R-parity violating models has been searched for at LEP [237]. Assuming fully leptonic decays via λ -type couplings, lower mass limits between 85 and 100 GeV are set. At the Tevatron [239, 240] and at the LHC [238, 241–243], searches have focused on scenarios with resonant production of a sneutrino decaying to $e\mu$, $\mu\tau$ and $e\tau$ final states. Limits have been set on sneutrino masses as a function of the value of relevant RPV couplings. As an example, the LHC experiments exclude a resonant tau sneutrino with a mass below 3.9 TeV for $\lambda_{312} = \lambda_{321} > 0.07$ and $\lambda'_{311} > 0.11$ [244].

Formulating a general assessment of the existing bounds on RPV SUSY models is becoming increasingly important in order to evaluate loopholes and potential new search directions. A classification of all potential RPV signatures at the LHC for small couplings has been recently published [245] to evaluate the coverage of the most general RPV-MSSM setup, without making any assumptions about the sparticle spectrum details. Small RPV couplings imply that sparticles are pair-produced at the LHC as in the RPC-MSSM case. Figure 88.10 shows a summary of the 95% C.L. limits on sparticle masses in RPV models for two types of λ couplings, compared to the direct production mass bound when the sparticle under consideration is the LSP. This is done to quantify the impact of possible assumptions made on the nature, mass and coupling choices for the LSP which in turn might lead to different leptons, jets and top-quark multiplicities. As underlined in [245], changes in exclusion limits on sparticle masses are at most around 20%.

Finally, RPV signatures are often similar to signatures of Stealth SUSY [246–248]. In these scenarios, squarks can decay to a quark and a chargino (neutralino), which can subsequently decay to a singlino \tilde{S} and a W^{\pm} (photon), with the \tilde{S} decaying to two gluons and a soft gravitino \tilde{G} . Dedicated CMS searches [249,250] exclude squark masses up to 1.85 TeV in the photon channel and up to 550 GeV in the charged lepton channel. Gluino masses up to 2.15 TeV are excluded in the di-photon channel [250]. Limits have also been placed on top squarks in stealth SUSY scenarios,

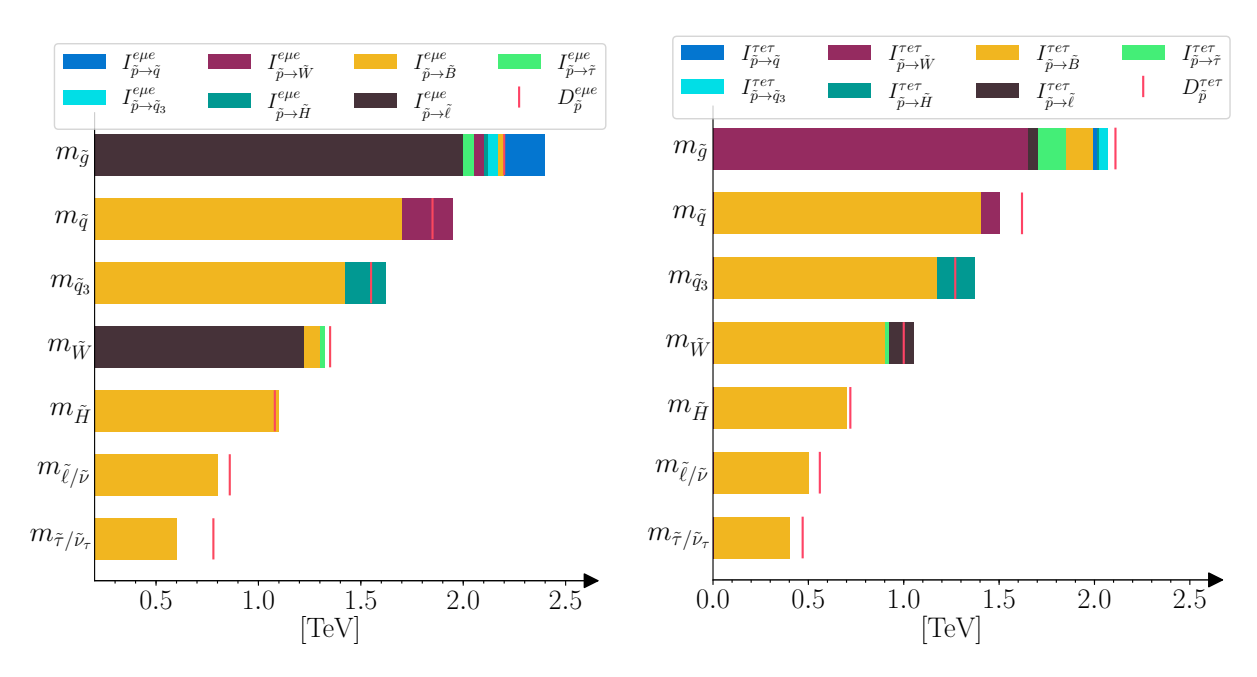


Figure 88.10: Summary of 95% C.L. limits on sparticle masses in RPV models, for λ_{121} (left), and for λ_{313} (right). The vertical red line represents the direct production mass bound when the sparticle under consideration is the LSP.

where the top squark decays to a top quark, a gluon and a \tilde{S} , and the \tilde{S} subsequently decays to a \tilde{G} and two gluons. In such a scenario, top squark masses up to 930 GeV have been excluded by CMS [232, 233].

88.9 Exclusion limits on long-lived sparticles

Long-lived sparticles arise in many different SUSY models. In particular in co-annihilation scenarios, where the NLSP and LSP are nearly mass-degenerate, this is rather common in order to obtain the correct Dark Matter relic density. Prominent examples are scenarios featuring stau co-annihilation, or models of SUSY breaking, e.g. minimal anomaly-mediated SUSY breaking (AMSB), in which the appropriate Dark Matter density is obtained by co-annihilation of the LSP with an almost degenerate long-lived wino. R-parity violating SUSY models might also lead to nonprompt decays. Searches for events with a displaced hadronic vertex, with or without a matched lepton, are for instance interpreted in a model with RPV neutralino decays involving a non-zero λ' coupling [235]. However, in general, other sparticles can also be long-lived and it is desirable to establish a comprehensive search program for these special long-lived cases, which lead to distinct experimental search signatures. Past experiments have performed dedicated searches for long-lived SUSY signatures, but given the absence of any experimental evidence for SUSY so far, more effort and focus has gone into searches for long-lived sparticles at the LHC recently. Signatures interpreted in terms of SUSY models include disappearing tracks, identification of tracks with atypical properties or unusual ionization, small and localized deposits of energy inside of the calorimeters without associated tracks, or stopped particles that decay out of time with collisions. Some examples are reported below with interpretations provided for gluinos, squarks and electroweak SUSY particles in a variety of SUSY models.

If the decay of gluinos is suppressed, for example if squark masses are high, gluinos may live longer than typical hadronization times. It is expected that such gluinos will hadronize to long-living strongly interacting particles known as R-hadrons. In particular, if the suppression of the gluino

decay is strong, as in the case that the squark masses are much higher than the TeV scale, these R-hadrons can be (semi-)stable in collider timescales. Searches for such R-hadrons exploit the typical signature of stable charged massive particles in the detector. R-hadrons decaying in the detector are searched for using dE/dx measurements and searches for displaced vertices. As shown in the left plot of Fig. 88.11, the ATLAS experiment excludes semi-stable gluino R-hadrons with masses below 1.9-2.3 TeV for all lifetimes in a simplified model where such gluinos always form R-hadrons, and decay into jets and a light neutralino, by combining a number of analyses [211, 251–254]. A combination of CMS searches for long-lived particles, as shown in Fig. 88.12, reaches similar limits [255–259].

Alternatively, since such R-hadrons are strongly interacting, they may be stopped in the calorimeter or in other material, and decay later into energetic jets. These decays are searched for by identifying the jets [260–262] or muons [262] outside the time window associated with bunch-bunch collisions. As shown in Fig. 88.12, the CMS collaboration sets limits on such stopped R-hadrons over 13 orders of magnitude in gluino lifetime, up to masses of 1390 GeV [262]. Recent results from ATLAS [263] sets constraints on the mass of gluino R-hadrons using large out-of-time energy deposits in the calorimeters. Also in this case, masses of up to 1.4 TeV are excluded for gluino lifetimes of $10^{-5} - 10^3$ s.

Top squarks can also be long-lived and hadronize to a R-hadron, for example in the scenario where the top squark is the next-to-lightest SUSY particle, with a small mass difference to the LSP. Searches for massive stable charged particles are sensitive to such top squarks. Tevatron limits are approximately $m_{\tilde{t}} > 300$ GeV [264, 265]. ATLAS sets a limit of 1340 GeV on such top squarks [253], the CMS limits are comparable [257]. Intermediate lifetimes of top squarks decaying through RPV coupling into a quark and a lepton are also targeted by ATLAS and CMS. Limits on top squarks decaying into a quark and a muon are set by ATLAS [266] using events that pass a muon or missing-transverse-momentum trigger and contain a displaced muon track and a displaced vertex. Masses up to 1.7 TeV are excluded for a lifetime of 0.1 ns, and masses below 1.3 TeV are excluded for lifetimes between 0.01 ns and 30 ns. CMS [267] utilizes events with two leptons with transverse impact parameter values between 0.01 and 10 cm not required to form a common vertex to exclude top squarks with masses between 100 and at least 460 GeV for $0.01 < c\tau_0 < 1000$ cm, where $c\tau_0$ is the proper decay length.

In addition to colored sparticles, sparticles like charginos may also be long-lived, especially in scenarios with compressed mass spectra. Charginos decaying in the detectors away from the primary vertex could lead to signatures such as kinked-tracks, or apparently disappearing tracks, since, for example, the pion in $\tilde{\chi}_1^{\pm} \to \pi^{\pm} \tilde{\chi}_1^0$ might be too soft to be reconstructed. At the LHC, searches have been performed for such disappearing tracks, and interpreted within anomaly-mediated SUSY breaking models [268–271]. The right plot of Fig. 88.11 shows constraints for different ATLAS searches on the chargino mass-vs-lifetime plane for an AMSB model (tan $\beta = 5$, $\mu > 0$) in which a wino-like $\tilde{\chi}^{\pm}$ decays to a soft pion and an almost mass-degenerated wino-like $\tilde{\chi}^{0}_{1}$ [253,254,269–272]. The disappearing track search [271] provides constraints also for higgsino-like models. Results from [272] exploiting anomalously large specific ionisation losses dE/dx are extrapolated to the stable regime. For a similar AMSB-like model, CMS excludes $c\tau$ values between 0.15 and 18 m for a chargino mass of 505 GeV [268], see Fig. 88.12. Their most recent results [273] expand and improve the constraints on masses of charginos as well as of colored sparticles (stop, sbottom, gluino) by making use of electron and muon plus disappearing track signatures, measurements of the dE/dx ionization energy loss of candidate tracks, and by re-analyzing the fully hadronic signatures using ML techniques. Bottom (top) squarks decaying to a long-lived chargino which results in a disappearing track signature are excluded below a mass of 900 - 1540 GeV (1100 -

1590 GeV), depending on the LSP mass and the chargino lifetime. Similarly, gluinos decaying to a long-lived chargino are excluded below a mass of 1450 - 2300 GeV, depending on LSP mass and chargino lifetime.

Charginos with a lifetime longer than the time needed to pass through the detector appear as charged stable massive particles. Limits have been derived by the LEP experiments [274], by D0 at the Tevatron [265], and by the LHC experiments [253,275], and such charginos with mass below 1090 GeV are excluded.

In gauge mediation models, NLSP neutralino decays need not be prompt, and experiments have searched for late decays with photons in the final state. CDF has searched for delayed $\tilde{\chi}_1^0 \to \gamma \tilde{G}$ decays using the timing of photon signals in the calorimeter [276]. CMS has used the same technique at the LHC [277]. Results are given as exclusion contours in the neutralino mass versus lifetime plane, and for example in a GMSB model with a neutralino mass of 300 GeV, $c\tau$ values between 10 and 2000 cm are excluded [277]. D0 has looked at the direction of showers in the electromagnetic calorimeter with a similar goal [278], and ATLAS has searched for photon candidates that do not point back to the primary vertex, as well as for delayed photons [279].

Charged slepton decays may be kinematically suppressed, for example in the scenario of a NLSP slepton with a very small mass difference to the LSP. Such a slepton may appear to be a stable charged massive particle. Interpretation of searches at LEP for such signatures within GMSB models with a stau NLSP or slepton co-NLSP exclude masses up to 99 GeV [274]. Searches for

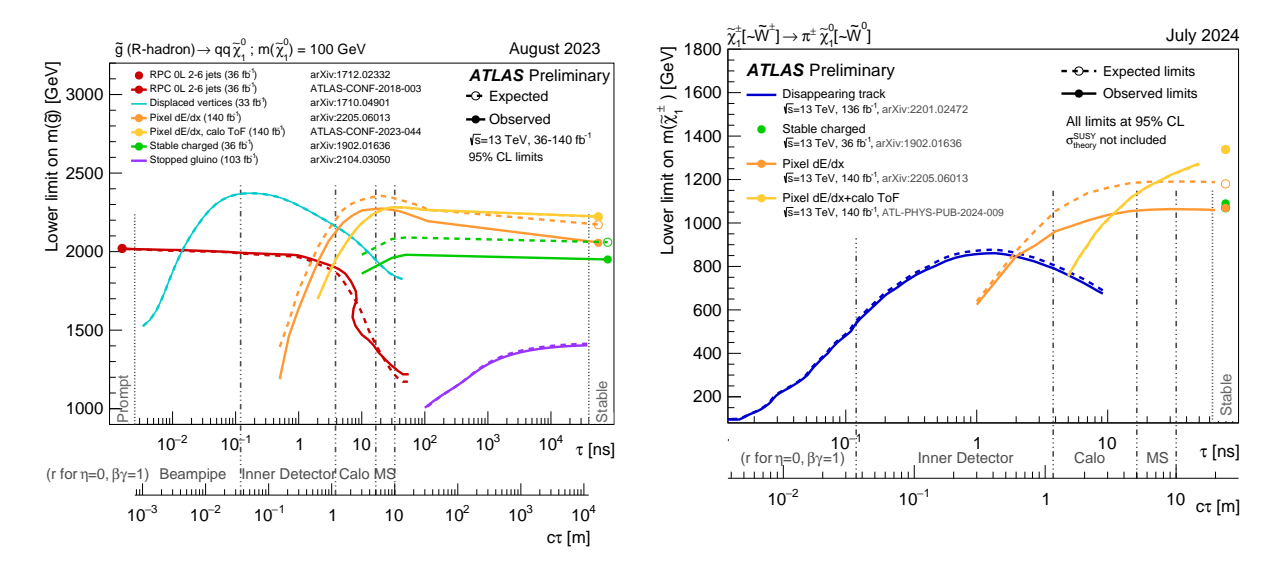


Figure 88.11: Limits at 95% C.L. on the gluino mass in R-hadron models (left), and on the chargino mass in a model where the wino-like chargino is almost degenerate with the LSP (right), as a function of gluino or chargino lifetime, as obtained by ATLAS.

stable charged particles at the Tevatron [264, 265] and at the LHC [253, 257] are also interpreted in terms of limits on stable charged sleptons. The limits obtained at the LHC exclude stable staus with masses below 430 GeV when produced directly in pairs, and below 660 GeV when staus are produced both directly and indirectly in the decay of other particles in a GMSB model. Recent results from ATLAS and CMS set constraints on long-lived charged sleptons with intermediate lifetimes. ATLAS searches for charged leptons with large impact parameters and exclude selectron, smuon and stau masses up to 720 GeV, 680 GeV, and 340 GeV, respectively, in case of lifetimes of 0.1 ns. They also exclude smuons with lifetimes down to 1 ps for a smuon mass of 100 GeV, and smuon masses up to 520 GeV are excluded for a proper lifetime of 10 ps [280]. CMS [197] targets

long-lived stau with $c\tau$ of about 0.1 mm excluding masses between 115 and 220 GeV for the case that the LSP is nearly massless.

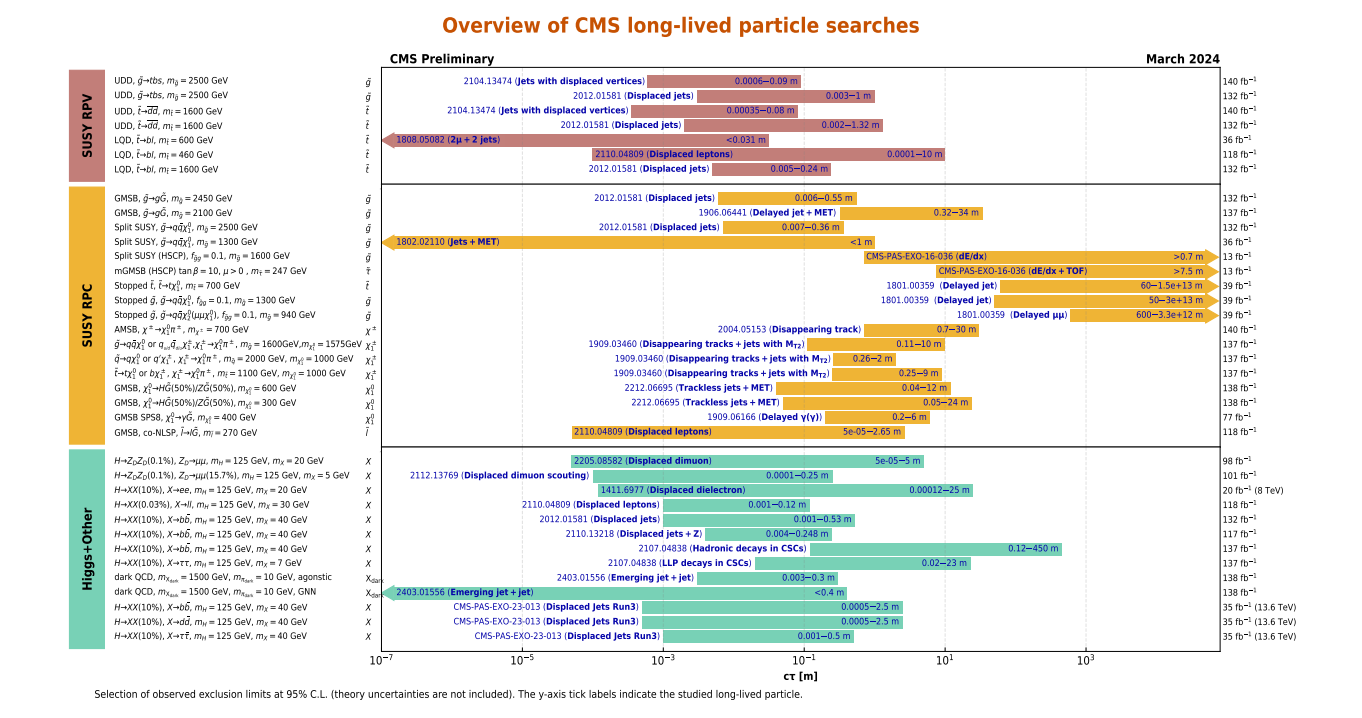


Figure 88.12: Excluded regions, at 95% C.L., in the lifetimes of long-lived particles in several models, as obtained by CMS.

88.10 Global interpretations

Apart from the interpretation of direct searches for sparticle production at colliders in terms of limits on masses of individual SUSY particles, model-dependent interpretations of allowed SUSY parameter space are derived from global SUSY fits. Typically these fits combine the results from collider experiments with indirect constraints on SUSY as obtained from low-energy experiments, flavor physics, high-precision electroweak results, and astrophysical data.

In the pre-LHC era these fits were mainly dominated by indirect constraints. Even for very constrained models like the CMSSM, the allowed parameter space, in terms of squark and gluino masses, ranged from several hundreds of GeV to a few TeV. Furthermore, these global fits indicated that squarks and gluino masses in the range of 500 to 1000 GeV were the preferred region of parameter space, although values as high as a few TeV were allowed with lower probabilities [281–288].

With ATLAS and CMS now probing mass scales around 1 TeV and beyond, the importance of the direct searches for global analyses of allowed SUSY parameter space has increased. For example, imposing the new experimental limits on constrained supergravity models pushes the most likely values of first generation squark and gluino masses significantly beyond 2 TeV, typically resulting in overall values of fit quality much worse than those in the pre-LHC era [158–160,188,289–296]. The measured value of m_h pushes the sparticle masses upwards. Although these constrained models are not yet ruled out, the extended experimental limits impose very tight constraints on the allowed parameter space.

For this reason, the emphasis of global SUSY fits has shifted towards less-constrained SUSY

models. Interpretations in the pMSSM [186–190, 275, 289, 297] as well as in simplified models, have been useful to generalize SUSY searches, for example to redesign experimental analyses in order to increase their sensitivity for compressed spectra, where the mass of the LSP is much closer to squark and gluino masses than predicted by the CMSSM. As shown in Table 88.1, for neutralino LSP masses above 0.5–1 TeV the current set of ATLAS and CMS searches, interpreted in simplified models, cannot exclude the existence of squarks or gluinos with masses only marginally above the neutralino mass. However, as these exclusion limits are defined in the context of simplified models, they are only valid for the assumptions in which these models are defined.

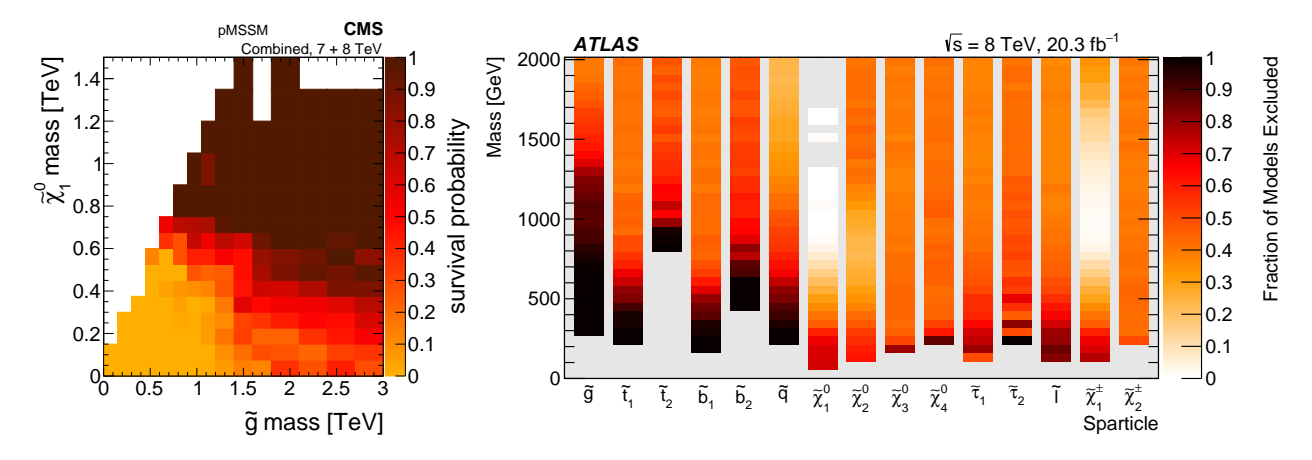


Figure 88.13: The plot on the left shows the survival probability of a pMSSM parameter space model in the gluino-neutralino mass plane after the application of the relevant CMS search results. The plot on the right shows a graphical representation of the ATLAS exclusion power in a pMSSM model. Each vertical bar is a one-dimensional projection of the fraction of models points excluded for each sparticle by ATLAS analyses. The experimental results are obtained from data taken at $\sqrt{s} = 7$ and 8 TeV.

Fig. 88.13 shows graphically the LHC exclusion power in the pMSSM based on searches performed at $\sqrt{s}=7$ and 8 TeV as reported by ATLAS [186] and CMS [187]. The plot on the left shows the survival probability in the gluino-neutralino mass plane, which is a measure of the parameter space that remains after inclusion of the relevant CMS search results. As can be seen, gluino masses below about 1.2 TeV are almost fully excluded. This result agrees well with the typical exclusion obtained at 8 TeV in simplified models for gluino production. However, as shown in the right plot of Fig. 88.13, when a similar analysis for other sparticles is performed it becomes apparent that exclusions on the pMSSM parameter can be significantly less stringent than simplified model limits might suggest.

More recently, the results of eight searches performed by ATLAS targeting the production of charginos and neutralinos, each using $\sqrt{s}=13\,$ TeV data, have been interpreted in the context of the 19-parameter R-parity conserving pMSSM where the LSP is assumed to be the lightest neutralino [191]. Constraints from previous electroweak, flavor and dark matter related measurements are also considered. The results are presented in terms of constraints on supersymmetric particle masses and are compared with limits from simplified models. Example spectra for non-excluded supersymmetric models with light charginos and neutralinos are also reported. This again indicates that care must be taken when interpreting results from the LHC searches and there are still several scenarios where sparticles below the 1 TeV scale are not excluded, even when considering the most recent results at $\sqrt{s}=13\,$ TeV.

Further interpretations in the pMSSM of searches performed on the full Run 2 dataset are in

preparation and will offer further insights on the validity of constraints obtained with simplified models and, thus, guidance towards the future LHC runs and beyond.

Finally, the discovery of a Higgs boson with a mass around 125 GeV has triggered many studies regarding the compatibility of SUSY parameter space with this new particle (see for example [298, 299]). Much of it is still work in progress and it will be interesting to see how the interplay between the results from direct SUSY searches and more precise measurements of the properties of the Higgs boson will unfold in the future.

88.11 Summary and Outlook

The absence of any observation of new phenomena at the first run of the LHC at $\sqrt{s} = 7/8$ TeV, and after the second run at $\sqrt{s} = 13$ TeV, places significant constraints on SUSY parameter space. An overview of the current landscape of SUSY searches and limits at the LHC is shown in Figure 88.14, where a summary of results from the ATLAS experiment [300] (CMS results are similar [301]), is reported for illustration purposes. Inclusive searches probe production of gluinos at about 2.45 TeV, first and second generation squarks in the range of about 1 to 1.9 TeV, third generation squarks at scales around 600 GeV to 1.2 TeV, electroweak gauginos at scales around 400 - 1100 GeV, and sleptons around 700 GeV. However, depending on the assumptions made on the underlying SUSY spectrum these limits can also weaken considerably.

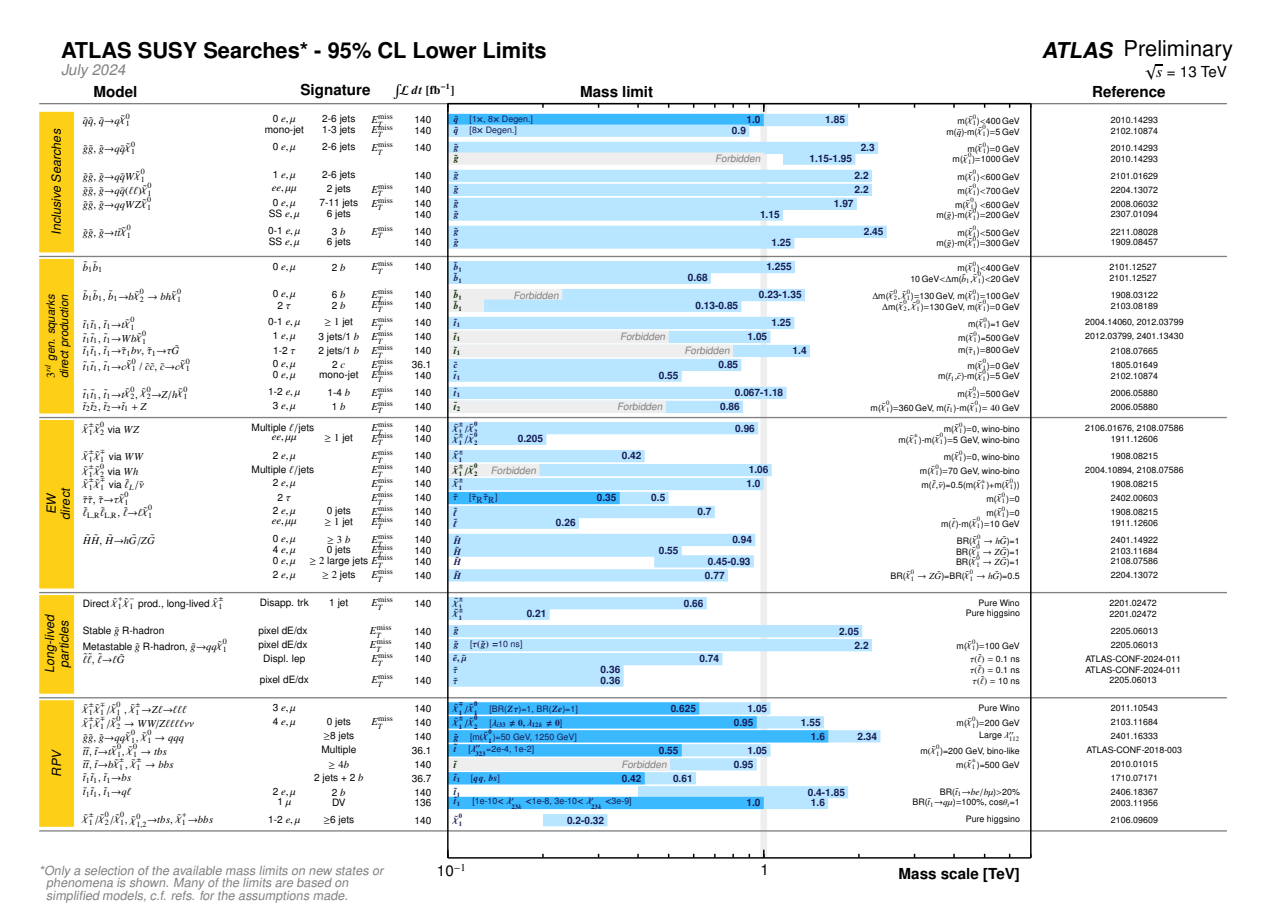


Figure 88.14: Overview of the current landscape of SUSY searches at the LHC (updated on August 2023). The plot shows exclusion mass limits of ATLAS for different searches and interpretation assumptions. The corresponding results of the CMS experiment are similar.

With the LHC having reached almost its maximum energy of about $\sqrt{s} = 14$ TeV and analyses

explored the full Run 2 dataset, future sensitivity improvements will have to originate from more data, the improvement of experimental analysis techniques and the focus on special signatures like the ones arising in long-lived sparticle decays. Therefore, it is expected that the current landscape of SUSY searches and corresponding exclusion limits at the LHC, especially for strongly produced sparticles in RPC scenarios, will not change as rapidly anymore as it did in the past, when the LHC underwent several successive increases of collision energy.

The interpretation of results at the LHC has moved away from constrained models like the CMSSM towards a large set of simplified models, or the pMSSM. Quoted limits in simplified models are only valid under the explicit assumptions made in these models. The addition of more comprehensive interpretations in the pMSSM complement those and therefore enable an even more refined understanding of the probed SUSY parameter space.

In this context, the limit range of 1.5-2.45 TeV on generic colored SUSY particles only holds for light neutralinos, in the R-parity conserving MSSM. Limits on third generation squarks and electroweak gauginos also only hold for light neutralinos, and under specific assumptions for decay modes and slepton masses. Constraints in R-parity violating SUSY models strongly depend also on the assumed non-zero couplings.

The next LHC runs, with \sqrt{s} between 13 and 14 TeV and significantly larger integrated luminosities (notably the High-Luminosity LHC), will provide a large data sample for future SUSY searches. As mentioned above, the improvement in sensitivity will largely have to come from a larger data set, and evolution of trigger and analysis techniques, since there will be no significant energy increase at the LHC anymore. Although the sensitivity for colored sparticles will increase somewhat as well, the expanded data set will be particularly beneficial for electroweak gaugino searches, and for the more difficult final states presented by compressed particle spectra, stealth SUSY, long-lived sparticles, or R-parity violating scenarios.

References

- [1] H. Miyazawa, Prog. Theor. Phys. **36**, 6, 1266 (1966).
- [2] Yu. A. Golfand and E. P. Likhtman, JETP Lett. **13**, 323 (1971), [Pisma Zh. Eksp. Teor. Fiz.13,452(1971)].
- [3] J.-L. Gervais and B. Sakita, Nucl. Phys. **B34**, 632 (1971).
- [4] D. V. Volkov and V. P. Akulov, Phys. Lett. **46B**, 109 (1973).
- [5] J. Wess and B. Zumino, Phys. Lett. **49B**, 52 (1974).
- [6] J. Wess and B. Zumino, Nucl. Phys. **B70**, 39 (1974).
- [7] A. Salam and J. A. Strathdee, Nucl. Phys. **B76**, 477 (1974).
- [8] H. P. Nilles, Phys. Rept. **110**, 1 (1984).
- [9] H. E. Haber and G. L. Kane, Phys. Rept. 117, 75 (1985).
- [10] E. Witten, Nucl. Phys. **B188**, 513 (1981).
- [11] S. Dimopoulos and H. Georgi, Nucl. Phys. **B193**, 150 (1981).
- [12] M. Dine, W. Fischler and M. Srednicki, Nucl. Phys. **B189**, 575 (1981).
- [13] S. Dimopoulos and S. Raby, Nucl. Phys. **B192**, 353 (1981).
- [14] N. Sakai, Z. Phys. C11, 153 (1981).
- [15] R. K. Kaul and P. Majumdar, Nucl. Phys. **B199**, 36 (1982).
- [16] H. Goldberg, Phys. Rev. Lett. **50**, 1419 (1983).
- [17] J. R. Ellis et al., Nucl. Phys. **B238**, 453 (1984).

- [18] G. Jungman, M. Kamionkowski and K. Griest, Phys. Rept. 267, 195 (1996), [hep-ph/9506380].
- [19] S. Dimopoulos, S. Raby and F. Wilczek, Phys. Rev. **D24**, 1681 (1981).
- [20] W. J. Marciano and G. Senjanovic, Phys. Rev. **D25**, 3092 (1982).
- [21] M. B. Einhorn and D. R. T. Jones, Nucl. Phys. **B196**, 475 (1982).
- [22] L. E. Ibanez and G. G. Ross, Phys. Lett. 105B, 439 (1981).
- [23] U. Amaldi, W. de Boer and H. Furstenau, Phys. Lett. **B260**, 447 (1991).
- [24] P. Langacker and N. Polonsky, Phys. Rev. **D52**, 3081 (1995), [hep-ph/9503214].
- [25] J. R. Ellis, S. Kelley and D. V. Nanopoulos, Phys. Lett. B 260, 131 (1991).
- [26] P. Fayet, Phys. Lett. **64B**, 159 (1976).
- [27] G. R. Farrar and P. Fayet, Phys. Lett. **76B**, 575 (1978).
- [28] B.C. Allanach and H.E. Haber, Supersymmetry, Part I (Theory), in this Review.
- [29] A. M. Sirunyan et al. (CMS), JHEP **04**, 188 (2020), [arXiv:1910.12127].
- [30] M. Aaboud et al. (ATLAS), JHEP **04**, 098 (2019), [arXiv:1812.03017].
- [31] R. Aaij et al. (LHCb), Phys. Rev. Lett. 118, 19, 191801 (2017), [arXiv:1703.05747].
- [32] A. Höcker and W.J. Marciano, Muon Anomalous Magnetic Moment, in this Review.
- [33] D. P. Aguillard et al. (Muon g-2) (2025), [arXiv:2506.03069].
- [34] G. Hinshaw et al. (WMAP), Astrophys. J. Suppl. 208, 19 (2013), [arXiv:1212.5226].
- [35] N. Aghanim *et al.* (Planck Collaboration), A&A **641**, A1 (2020).
- [36] K. Nakamura et al. (Particle Data Group), J. Phys. **G37**, 075021 (2010).
- [37] I. Hinchliffe et al., Phys. Rev. **D55**, 5520 (1997), [hep-ph/9610544].
- [38] L. Randall and D. Tucker-Smith, Phys. Rev. Lett. 101, 221803 (2008), [arXiv:0806.1049].
- [39] V. Khachatryan et al. (CMS), Phys. Lett. **B698**, 196 (2011), [arXiv:1101.1628].
- [40] S. Chatrchyan et al. (CMS), Phys. Rev. Lett. 107, 221804 (2011), [arXiv:1109.2352].
- [41] S. Chatrchyan et al. (CMS), JHEP 01, 077 (2013), [arXiv:1210.8115].
- [42] S. Chatrchyan et al. (CMS), Eur. Phys. J. C73, 9, 2568 (2013), [arXiv:1303.2985].
- [43] S. Chatrchyan et al. (CMS), Phys. Rev. **D85**, 012004 (2012), [arXiv:1107.1279].
- [44] C. G. Lester and D. J. Summers, Phys. Lett. **B463**, 99 (1999), [hep-ph/9906349].
- [45] D. R. Tovey, JHEP **04**, 034 (2008), [arXiv:0802.2879].
- [46] M. R. Buckley et al., Phys. Rev. **D89**, 5, 055020 (2014), [arXiv:1310.4827].
- [47] P. Jackson, C. Rogan and M. Santoni, Phys. Rev. **D95**, 3, 035031 (2017), [arXiv:1607.08307].
- [48] G. Aad et al. (ATLAS), Eur. Phys. J. C 81, 4, 334 (2021), [arXiv:2009.04986].
- [49] J. M. Butterworth et al., Phys. Rev. Lett. 100, 242001 (2008), [arXiv:0802.2470].
- [50] A. M. Sirunyan et al. (CMS), JINST 15, 06, P06005 (2020), [arXiv:2004.08262].
- [51] A. M. Sirunyan et al. (CMS), JHEP **05**, 032 (2020), [arXiv:1912.08887].
- [52] N. Arkani-Hamed and S. Dimopoulos, JHEP **06**, 073 (2005), [hep-th/0405159].
- [53] G. F. Giudice and A. Romanino, Nucl. Phys. B 699, 65 (2004), [Erratum: Nucl.Phys.B 706, 487–487 (2005)], [hep-ph/0406088].
- [54] J. Alimena et al., J. Phys. G 47, 9, 090501 (2020), [arXiv:1903.04497].
- [55] A.H. Chamseddine, R. Arnowitt, and P Nath, Phys. Rev. Lett. 49, 970 (1982).

- [56] E. Cremmer et al., Nucl. Phys. **B212**, 413 (1983).
- [57] P. Fayet, Phys. Lett. **70B**, 461 (1977).
- [58] M. Dine, A. E. Nelson and Y. Shirman, Phys. Rev. **D51**, 1362 (1995), [hep-ph/9408384].
- [59] P. Meade, N. Seiberg and D. Shih, Prog. Theor. Phys. Suppl. 177, 143 (2009), [arXiv:0801.3278].
- [60] G. F. Giudice et al., JHEP 12, 027 (1998), [hep-ph/9810442].
- [61] L. Randall and R. Sundrum, Nucl. Phys. **B557**, 79 (1999), [hep-th/9810155].
- [62] R. L. Arnowitt and P. Nath, Phys. Rev. Lett. 69, 725 (1992).
- [63] G. L. Kane et al., Phys. Rev. **D49**, 6173 (1994), [hep-ph/9312272].
- [64] A. Djouadi et al. (MSSM Working Group), in "GDR (Groupement De Recherche) Supersymetrie," (1998), [hep-ph/9901246].
- [65] A. Djouadi, J.-L. Kneur and G. Moultaka, Comput. Phys. Commun. 176, 426 (2007), [hep-ph/0211331].
- [66] C. F. Berger *et al.*, JHEP **02**, 023 (2009), [arXiv:0812.0980].
- [67] H. Baer et al., in "Workshop on Physics at Current Accelerators and the Supercollider Argonne, Illinois, June 2-5, 1993," 0703-720 (1993), [hep-ph/9305342], URL http://lss.fnal.gov/cgi-bin/find_paper.pl?other/ssc/sscl-preprint-441.
- [68] R. M. Barnett, H. E. Haber and G. L. Kane, Nucl. Phys. **B267**, 625 (1986).
- [69] H. Baer, D. Karatas and X. Tata, Phys. Lett. **B183**, 220 (1987).
- [70] J. Alwall, P. Schuster and N. Toro, Phys. Rev. **D79**, 075020 (2009), [arXiv:0810.3921].
- [71] J. Alwall et al., Phys. Rev. **D79**, 015005 (2009), [arXiv:0809.3264].
- [72] LEP2 SUSY Working Group, ALEPH, DELPHI, L3 and OPAL experiments, note LEPSUSYWG/04-02.1, http://lepsusy.web.cern.ch/lepsusy.
- [73] LHC SUSY cross sections working group, https://twiki.cern.ch/twiki/bin/view/LHCPhysics/SUSYCrossSections.
- [74] T. Aaltonen et al. (CDF), Phys. Rev. Lett. 102, 121801 (2009), [arXiv:0811.2512].
- [75] V. M. Abazov et al. (D0), Phys. Lett. **B660**, 449 (2008), [arXiv:0712.3805].
- [76] A. M. Sirunyan et al. (CMS) (2019), [arXiv:1908.04722].
- [77] ATLAS Collab., ATLAS-CONF-2019-040 (2019).
- [78] G. Aad et al. (ATLAS), Eur. Phys. J. C 81, 7, 600 (2021), [arXiv:2101.01629].
- [79] G. Aad et al. (ATLAS), JHEP **02**, 143 (2021), [arXiv:2010.14293].
- [80] A. Tumasyan et al. (CMS), JHEP **09**, 149 (2023), [arXiv:2211.08476].
- [81] A. M. Sirunyan et al. (CMS), JHEP 10, 244 (2019), [arXiv:1908.04722].
- [82] G. Aad et al. (ATLAS), Eur. Phys. J. C 83, 7, 561 (2023), [arXiv:2211.08028].
- [83] ATLAS Collab., ATLAS-CONF-2018-041 (2018).
- [84] A. M. Sirunyan et al. (CMS), Eur. Phys. J. C 80, 1, 3 (2020), [arXiv:1909.03460].
- [85] A. M. Sirunyan et al. (CMS), Phys. Rev. D 104, 5, 052001 (2021), [arXiv:2103.01290].
- [86] G. Aad et al. (ATLAS Collaboration), Phys. Rev. D 103, 112006 (2021), URL https://link.aps.org/doi/10.1103/PhysRevD.103.112006.
- [87] M. Aaboud et al. (ATLAS), Phys. Rev. D 97, 9, 092006 (2018), [arXiv:1802.03158].
- [88] G. Aad et al. (ATLAS), Eur. Phys. J. C 83, 6, 515 (2023), [arXiv:2204.13072].

- [89] G. Aad et al. (ATLAS), JHEP **02**, 107 (2024), [arXiv:2307.01094].
- [90] M. Aaboud et al. (ATLAS), JHEP **09**, 050 (2018), [arXiv:1805.01649].
- [91] G. Aad et al. (ATLAS), JHEP **02**, 193 (2025), [arXiv:2410.17824].
- [92] T. Aaltonen et al. (CDF), Phys. Rev. Lett. 105, 081802 (2010), [arXiv:1005.3600].
- [93] V. M. Abazov et al. (D0), Phys. Lett. **B693**, 95 (2010), [arXiv:1005.2222].
- [94] G. Aad et al. (ATLAS), JHEP **05**, 093 (2021), [arXiv:2101.12527].
- [95] G. Aad et al. (ATLAS), JHEP 12, 060 (2019), [arXiv:1908.03122].
- [96] G. Aad et al. (ATLAS), JHEP **06**, 046 (2020), [arXiv:1909.08457].
- [97] G. Aad et al. (ATLAS), Phys. Rev. D 104, 3, 032014 (2021), [arXiv:2103.08189].
- [98] A. M. Sirunyan et al. (CMS), JHEP **03**, 076 (2018), [arXiv:1709.08908].
- [99] A. M. Sirunyan et al. (CMS), Eur. Phys. J. C 80, 8, 752 (2020), [arXiv:2001.10086].
- [100] C. Boehm, A. Djouadi and Y. Mambrini, Phys. Rev. **D61**, 095006 (2000), [hep-ph/9907428].
- [101] T. Aaltonen et al. (CDF), Phys. Rev. **D82**, 092001 (2010), [arXiv:1009.0266].
- [102] V. M. Abazov et al. (D0), Phys. Lett. **B696**, 321 (2011), [arXiv:1009.5950].
- [103] T. Aaltonen et al. (CDF), JHEP 10, 158 (2012), [arXiv:1203.4171].
- [104] V. M. Abazov et al. (D0), Phys. Lett. **B665**, 1 (2008), [arXiv:0803.2263].
- [105] T. Aaltonen et al. (CDF), Phys. Rev. Lett. 104, 251801 (2010), [arXiv:0912.1308].
- [106] V. M. Abazov et al. (D0), Phys. Lett. **B674**, 4 (2009), [arXiv:0901.1063].
- [107] G. Aad et al. (ATLAS), Eur. Phys. J. C 80, 8, 737 (2020), [arXiv:2004.14060].
- [108] G. Aad et al. (ATLAS), JHEP **04**, 174 (2021), [arXiv:2012.03799].
- [109] Technical report, CERN, Geneva (2023), all figures including auxiliary figures are available at https://atlas.web.cern.ch/Atlas/GROUPS/PHYSICS/CONFNOTES/ATLAS-CONF-2023-043, URL https://cds.cern.ch/record/2869241.
- [110] M. Aaboud et al. (ATLAS), JHEP **06**, 108 (2018), [arXiv:1711.11520].
- [111] M. Aaboud et al. (ATLAS), Phys. Rev. **D98**, 3, 032008 (2018), [arXiv:1803.10178].
- [112] A. M. Sirunyan et al. (CMS), JHEP **02**, 015 (2020), [arXiv:1910.12932].
- [113] G. Aad et al. (ATLAS), JHEP **04**, 165 (2021), [arXiv:2102.01444].
- [114] A. M. Sirunyan et al. (CMS), Eur. Phys. J. C77, 10, 710 (2017), [arXiv:1705.04650].
- [115] A. M. Sirunyan et al. (CMS), Phys. Rev. **D96**, 3, 032003 (2017), [arXiv:1704.07781].
- [116] A. M. Sirunyan et al. (CMS), JHEP 10, 005 (2017), [arXiv:1707.03316].
- [117] A. M. Sirunyan et al. (CMS), JHEP 10, 019 (2017), [arXiv:1706.04402].
- [118] A. M. Sirunyan et al. (CMS), Eur. Phys. J. C 81, 1, 3 (2021), [arXiv:2008.05936].
- [119] A. M. Sirunyan et al. (CMS), JHEP **03**, 101 (2019), [arXiv:1901.01288].
- [120] A. Tumasyan et al. (CMS), JHEP **07**, 110 (2023), [arXiv:2304.07174].
- [121] M. Aaboud et al. (ATLAS), Phys. Rev. D 98, 3, 032008 (2018), [arXiv:1803.10178].
- [122] G. Aad et al. (ATLAS), Phys. Rev. D 104, 11, 112005 (2021), [arXiv:2108.07665].
- [123] G. Aad et al. (ATLAS), Eur. Phys. J. C 80, 11, 1080 (2020), [arXiv:2006.05880].
- [124] G. Aad et al. (ATLAS), JHEP 07, 250 (2024), [arXiv:2402.12137].
- [125] A. Tumasyan et al. (CMS), JHEP **06**, 060 (2023), [arXiv:2301.08096].
- [126] M. Aaboud et al. (ATLAS), Eur. Phys. J. C 80, 8, 754 (2020), [arXiv:1903.07570].

- [127] B. Fuks et al., JHEP 10, 081 (2012), [arXiv:1207.2159].
- [128] B. Fuks et al., Eur. Phys. J. C 73, 2480 (2013), [arXiv:1304.0790].
- [129] LEP2 SUSY Working Group, ALEPH, DELPHI, L3 and OPAL experiments, note LEPSUSYWG/01-03.1, http://lepsusy.web.cern.ch/lepsusy.
- [130] LEP2 SUSY Working Group, ALEPH, DELPHI, L3 and OPAL experiments, note LEPSUSYWG/02-04.1, http://lepsusy.web.cern.ch/lepsusy.
- [131] CDF Collab., CDF Note 10636 (2011).
- [132] V. M. Abazov et al. (D0), Phys. Lett. **B680**, 34 (2009), [arXiv:0901.0646].
- [133] G. Aad et al. (ATLAS), Eur. Phys. J. C 80, 2, 123 (2020), [arXiv:1908.08215].
- [134] A. M. Sirunyan et al. (CMS), JHEP 11, 079 (2018), [arXiv:1807.07799].
- [135] G. Aad et al. (ATLAS), JHEP 05, 150 (2024), [arXiv:2402.00603].
- [136] A. M. Sirunyan et al. (CMS), JHEP 11, 151 (2018), [arXiv:1807.02048].
- [137] G. Aad et al. (ATLAS), Phys. Rev. Lett. 133, 3, 031802 (2024), [arXiv:2402.08347].
- [138] G. Aad et al. (ATLAS), JHEP **06**, 031 (2023), [arXiv:2209.13935].
- [139] G. Aad et al. (ATLAS), JHEP 12, 167 (2023), [arXiv:2310.08171].
- [140] G. Aad et al. (ATLAS), Phys. Rev. D 104, 11, 112010 (2021), [arXiv:2108.07586].
- [141] A. Tumasyan et al. (CMS), Phys. Lett. B 842, 137460 (2023), [arXiv:2205.09597].
- [142] M. Aaboud et al. (ATLAS), Eur. Phys. J. C78, 12, 995 (2018), [arXiv:1803.02762].
- [143] A. Tumasyan et al. (CMS), JHEP **04**, 147 (2022), [arXiv:2106.14246].
- [144] A. Hayrapetyan et al. (CMS), Phys. Rev. D 109, 11, 112001 (2024), [arXiv:2402.01888].
- [145] G. Aad et al. (ATLAS), Eur. Phys. J. C 81, 12, 1118 (2021), [arXiv:2106.01676].
- [146] G. Aad et al. (ATLAS), JHEP 11, 150 (2023), [arXiv:2305.09322].
- [147] A. Tumasyan et al. (CMS), JHEP 10, 045 (2021), [arXiv:2107.12553].
- [148] M. Aaboud et al. (ATLAS), Phys. Rev. **D100**, 1, 012006 (2019), [arXiv:1812.09432].
- [149] G. Aad et al. (ATLAS), JHEP 10, 005 (2020), [arXiv:2004.10894].
- [150] G. Aad et al. (ATLAS), Eur. Phys. J. C 80, 8, 691 (2020), [arXiv:1909.09226].
- [151] G. Aad et al. (ATLAS), Phys. Rev. D 101, 5, 052005 (2020), [arXiv:1911.12606].
- [152] A. Tumasyan et al. (CMS), JHEP **04**, 091 (2022), [arXiv:2111.06296].
- [153] G. Aad et al. (ATLAS), JHEP 12, 116 (2024), [arXiv:2409.18762].
- [154] A. M. Sirunyan et al. (CMS), JHEP 08, 150 (2019), [arXiv:1905.13059].
- [155] A. M. Sirunyan et al. (CMS), Phys. Rev. Lett. **124**, 4, 041803 (2020), [arXiv:1910.01185].
- [156] H. K. Dreiner et al., Eur. Phys. J. C62, 547 (2009), [arXiv:0901.3485].
- [157] LEP2 SUSY Working Group, ALEPH, DELPHI, L3 and OPAL experiments, note LEPSUSYWG/04-07.1, http://lepsusy.web.cern.ch/lepsusy.
- [158] O. Buchmueller et al., Eur. Phys. J. C74, 6, 2922 (2014), [arXiv:1312.5250].
- [159] C. Strege et al., JCAP **1304**, 013 (2013), [arXiv:1212.2636].
- [160] A. Fowlie et al., Phys. Rev. **D86**, 075010 (2012), [arXiv:1206.0264].
- [161] LEP2 SUSY Working Group, ALEPH, DELPHI, L3 and OPAL experiments, note LEPSUSYWG/04-09.1, http://lepsusy.web.cern.ch/lepsusy.
- [162] T. Aaltonen et al. (CDF), Phys. Rev. Lett. 104, 011801 (2010), [arXiv:0910.3606].

- [163] V. M. Abazov et al. (D0), Phys. Rev. Lett. 105, 221802 (2010), [arXiv:1008.2133].
- [164] M. Aaboud et al. (ATLAS), Phys. Rev. **D97**, 9, 092006 (2018), [arXiv:1802.03158].
- [165] A. M. Sirunyan et al. (CMS), JHEP 06, 143 (2019), [arXiv:1903.07070].
- [166] A. M. Sirunyan et al. (CMS), Phys. Lett. B 801, 135183 (2020), [arXiv:1907.00857].
- [167] A. Hayrapetyan et al. (CMS), JHEP 10, 046 (2023), [arXiv:2307.16216].
- [168] M. Aaboud et al. (ATLAS), Phys. Rev. **D98**, 9, 092002 (2018), [arXiv:1806.04030].
- [169] M. Aaboud et al. (ATLAS), Phys. Rev. **D98**, 3, 032009 (2018), [arXiv:1804.03602].
- [170] M. Aaboud et al. (ATLAS), Phys. Rev. **D99**, 1, 012001 (2019), [arXiv:1808.03057].
- [171] G. Aad et al. (ATLAS), Phys. Rev. D 104, 11, 112010 (2021), [arXiv:2108.07586].
- [172] A. M. Sirunyan et al. (CMS), JHEP 03, 166 (2018), [arXiv:1709.05406].
- [173] A. M. Sirunyan et al. (CMS), JHEP **03**, 160 (2018), [arXiv:1801.03957].
- [174] A. M. Sirunyan et al. (CMS), Eur. Phys. J. C79, 5, 444 (2019), [arXiv:1901.06726].
- [175] A. M. Sirunyan et al. (CMS), JHEP **01**, 154 (2019), [arXiv:1812.04066].
- [176] A. M. Sirunyan et al. (CMS), Phys. Lett. **B780**, 118 (2018), [arXiv:1711.08008].
- [177] A. M. Sirunyan et al. (CMS), Phys. Rev. **D97**, 3, 032007 (2018), [arXiv:1709.04896].
- [178] A. M. Sirunyan et al. (CMS), Phys. Lett. **B779**, 166 (2018), [arXiv:1709.00384].
- [179] A. Tumasyan et al. (CMS), JHEP **05**, 014 (2022), [arXiv:2201.04206].
- [180] G. Aad et al. (ATLAS), Phys. Rev. **D93**, 5, 052002 (2016), [arXiv:1509.07152].
- [181] N. L. Rodd, B. R. Safdi and W. L. Xu, Phys. Rev. D 110, 4, 043003 (2024).
- [182] M. Aaboud et al. (ATLAS), Eur. Phys. J. C78, 8, 625 (2018), [arXiv:1805.11381].
- [183] M. Aaboud et al. (ATLAS), Eur. Phys. J. C77, 3, 144 (2017), [arXiv:1611.05791].
- [184] A. M. Sirunyan et al. (CMS), JHEP **04**, 123 (2021), [arXiv:2012.08600].
- [185] A. Arbey, M. Battaglia and F. Mahmoudi, Eur. Phys. J. C 72, 1847 (2012), [arXiv:1110.3726].
- [186] G. Aad et al. (ATLAS), JHEP 10, 134 (2015), [arXiv:1508.06608].
- [187] V. Khachatryan et al. (CMS), JHEP 10, 129 (2016), [arXiv:1606.03577].
- [188] P. Athron et al. (GAMBIT), Eur. Phys. J. C77, 12, 879 (2017), [arXiv:1705.07917].
- [189] K. J. de Vries et al., Eur. Phys. J. C75, 9, 422 (2015), [arXiv:1504.03260].
- [190] C. Strege et al., JHEP 09, 081 (2014), [arXiv:1405.0622].
- [191] G. Aad et al. (ATLAS), JHEP 05, 106 (2024), [arXiv:2402.01392].
- [192] LEP2 SUSY Working Group, ALEPH, DELPHI, L3 and OPAL experiments, note LEPSUSYWG/04-01.1, http://lepsusy.web.cern.ch/lepsusy.
- [193] A. Heister et al. (ALEPH), Phys. Lett. **B544**, 73 (2002), [hep-ex/0207056].
- [194] A. M. Sirunyan et al. (CMS), Phys. Lett. **B790**, 140 (2019), [arXiv:1806.05264].
- [195] G. Aad et al. (ATLAS), JHEP 08, 053 (2025), [arXiv:2503.17186].
- [196] A. M. Sirunyan et al. (CMS), Eur. Phys. J. C 80, 3, 189 (2020), [arXiv:1907.13179].
- [197] A. Tumasyan et al. (CMS), Phys. Rev. D 108, 1, 012011 (2023), [arXiv:2207.02254].
- [198] LEP2 SUSY Working Group, ALEPH, DELPHI, L3 and OPAL experiments, note LEPSUSYWG/02-09.2, http://lepsusy.web.cern.ch/lepsusy.
- [199] M. Aaboud et al. (ATLAS), Phys. Rev. **D99**, 1, 012009 (2019), [arXiv:1808.06358].
- [200] S. Chatrchyan et al. (CMS), Eur. Phys. J. C73, 2493 (2013), [arXiv:1301.3792].

- [201] S. Chatrchyan et al. (CMS), Phys. Rev. **D90**, 032006 (2014), [arXiv:1404.5801].
- [202] T. Aaltonen et al. (CDF), Phys. Rev. Lett. 110, 20, 201802 (2013), [arXiv:1302.4491].
- [203] DELPHI Collab., Eur. Phys. J. C31, 412 (2003).
- [204] G. Aad et al. (ATLAS), JHEP 07, 167 (2021), [arXiv:2103.11684].
- [205] M. Aaboud et al. (ATLAS), JHEP **09**, 084 (2017), [arXiv:1706.03731].
- [206] CMS Collab., CMS-PAS-SUS-19-008 (2019).
- [207] V. Khachatryan et al. (CMS), Phys. Rev. **D94**, 11, 112009 (2016), [arXiv:1606.08076].
- [208] CMS Collab., CMS-PAS-SUS-13-010 (2013).
- [209] T. Aaltonen et al. (CDF), Phys. Rev. Lett. 107, 042001 (2011), [arXiv:1105.2815].
- [210] M. Aaboud et al. (ATLAS), Phys. Lett. **B785**, 136 (2018), [arXiv:1804.03568].
- [211] ATLAS Collab., ATLAS-CONF-2018-003 (2018).
- [212] ATLAS Collab., ATLAS-CONF-2016-057 (2016).
- [213] M. Aaboud et al. (ATLAS), JHEP 09, 088 (2017), [arXiv:1704.08493].
- [214] A. M. Sirunyan et al. (CMS), Phys. Lett. **B783**, 114 (2018), [arXiv:1712.08920].
- [215] S. Chatrchyan et al. (CMS), Phys. Lett. **B730**, 193 (2014), [arXiv:1311.1799].
- [216] V. Khachatryan et al. (CMS), Phys. Lett. **B770**, 257 (2017), [arXiv:1608.01224].
- [217] G. Aad et al. (ATLAS), Eur. Phys. J. C 81, 11, 1023 (2021), [arXiv:2106.09609].
- [218] F. D. Aaron et al. (H1), Eur. Phys. J. C71, 1572 (2011), [arXiv:1011.6359].
- [219] ATLAS Collab., ATLAS-CONF-2015-018 (2015).
- [220] S. Chekanov et al. (ZEUS), Eur. Phys. J. C50, 269 (2007), [hep-ex/0611018].
- [221] M. Aaboud et al. (ATLAS), Phys. Rev. **D97**, 3, 032003 (2018), [arXiv:1710.05544].
- [222] G. Aad et al. (ATLAS), Phys. Rev. D 110, 9, 092004 (2024), [arXiv:2406.18367].
- [223] ATLAS Collab., ATLAS-CONF-2019-006 (2019).
- [224] A. M. Sirunyan et al. (CMS), Phys. Rev. **D99**, 3, 032014 (2019), [arXiv:1808.05082].
- [225] CMS Collab., CMS-PAS-EXO-16-022 (2016).
- [226] V. Khachatryan et al. (CMS), Phys. Lett. **B760**, 178 (2016), [arXiv:1602.04334].
- [227] M. Aaboud et al. (ATLAS), Eur. Phys. J. C 78, 3, 250 (2018), [arXiv:1710.07171].
- [228] M. Aaboud et al. (ATLAS), Eur. Phys. J. C78, 3, 250 (2018), [arXiv:1710.07171].
- [229] V. Khachatryan et al. (CMS), Phys. Rev. **D95**, 1, 012009 (2017), [arXiv:1610.05133].
- [230] V. Khachatryan et al. (CMS), Phys. Lett. **B747**, 98 (2015), [arXiv:1412.7706].
- [231] G. Aad *et al.* (ATLAS), Eur. Phys. J. C **81**, 1, 11 (2021), [Erratum: Eur.Phys.J.C 81, 249 (2021)], [arXiv:2010.01015].
- [232] A. M. Sirunyan et al. (CMS), Phys. Rev. D 104, 3, 032006 (2021), [arXiv:2102.06976].
- [233] V. Chekhovsky et al. (CMS) (2025), [arXiv:2506.08825].
- [234] G. Aad et al. (ATLAS), Phys. Rev. **D92**, 7, 072004 (2015), [arXiv:1504.05162].
- [235] V. Khachatryan et al. (CMS), Phys. Rev. **D91**, 1, 012007 (2015), [arXiv:1411.6530].
- [236] G. Aad et al. (ATLAS), Phys. Rev. D 103, 112003 (2021), [arXiv:2011.10543].
- [237] LEP2 SUSY Working Group, ALEPH, DELPHI, L3 and OPAL experiments, note LEPSUSYWG/02-10.1, http://lepsusy.web.cern.ch/lepsusy.
- [238] A. M. Sirunyan et al. (CMS), Eur. Phys. J. C79, 4, 305 (2019), [arXiv:1811.09760].

- [239] T. Aaltonen et al. (CDF), Phys. Rev. Lett. 105, 191801 (2010), [arXiv:1004.3042].
- [240] V. M. Abazov et al. (D0), Phys. Rev. Lett. 105, 191802 (2010), [arXiv:1007.4835].
- [241] G. Aad et al. (ATLAS), Phys. Rev. Lett. 115, 3, 031801 (2015), [arXiv:1503.04430].
- [242] M. Aaboud et al. (ATLAS), Eur. Phys. J. C76, 10, 541 (2016), [arXiv:1607.08079].
- [243] V. Khachatryan et al. (CMS), Eur. Phys. J. C76, 6, 317 (2016), [arXiv:1604.05239].
- [244] G. Aad et al. (ATLAS), JHEP 23, 082 (2020), [arXiv:2307.08567].
- [245] H. K. Dreiner et al., JHEP 07, 215 (2023), [arXiv:2306.07317].
- [246] J. Fan, M. Reece and J. T. Ruderman, JHEP 11, 012 (2011), [arXiv:1105.5135].
- [247] J. Fan, M. Reece and J. T. Ruderman, JHEP 07, 196 (2012), [arXiv:1201.4875].
- [248] J. Fan et al., JHEP 07, 016 (2016), [arXiv:1512.05781].
- [249] V. Khachatryan et al. (CMS), Phys. Lett. B **743**, 503 (2015), [arXiv:1411.7255].
- [250] A. Hayrapetyan et al. (CMS), Phys. Rev. D 109, 11, 112009 (2024), [arXiv:2310.03154].
- [251] Technical report, CERN, Geneva (2023), all figures including auxiliary figures are available at https://atlas.web.cern.ch/Atlas/GROUPS/PHYSICS/CONFNOTES/ATLAS-CONF-2023-044, URL https://cds.cern.ch/record/2870112.
- [252] M. Aaboud et al. (ATLAS), Phys. Rev. **D97**, 5, 052012 (2018), [arXiv:1710.04901].
- [253] M. Aaboud et al. (ATLAS), Phys. Rev. **D99**, 9, 092007 (2019), [arXiv:1902.01636].
- [254] G. Aad et al. (ATLAS), Eur. Phys. J. C75, 9, 407 (2015), [arXiv:1506.05332].
- [255] A. M. Sirunyan et al. (CMS), Phys. Lett. **B797**, 134876 (2019), [arXiv:1906.06441].
- [256] A. M. Sirunyan et al. (CMS), JHEP **05**, 025 (2018), [arXiv:1802.02110].
- [257] CMS Collab., CMS-PAS-EXO-16-036 (2016).
- [258] A. M. Sirunyan et al. (CMS), Phys. Lett. B 806, 135502 (2020), [arXiv:2004.05153].
- [259] A. M. Sirunyan et al. (CMS), Phys. Rev. D 104, 1, 012015 (2021), [arXiv:2012.01581].
- [260] V. M. Abazov et al. (D0), Phys. Rev. Lett. 99, 131801 (2007), [arXiv:0705.0306].
- [261] G. Aad et al. (ATLAS), Phys. Rev. **D88**, 11, 112003 (2013), [arXiv:1310.6584].
- [262] A. M. Sirunyan et al. (CMS), JHEP **05**, 127 (2018), [arXiv:1801.00359].
- [263] G. Aad et al. (ATLAS), JHEP 07, 173 (2021), [arXiv:2104.03050].
- [264] T. Aaltonen et al. (CDF), Phys. Rev. Lett. 103, 021802 (2009), [arXiv:0902.1266].
- [265] V. M. Abazov et al. (D0), Phys. Rev. **D87**, 5, 052011 (2013), [arXiv:1211.2466].
- [266] G. Aad et al. (ATLAS), Phys. Rev. D 102, 3, 032006 (2020), [arXiv:2003.11956].
- [267] A. Tumasyan et al. (CMS), Eur. Phys. J. C 82, 2, 153 (2022), [arXiv:2110.04809].
- [268] A. M. Sirunyan et al. (CMS), JHEP 08, 016 (2018), [arXiv:1804.07321].
- [269] M. Aaboud et al. (ATLAS), JHEP 06, 022 (2018), [arXiv:1712.02118].
- [270] G. Aad et al. (ATLAS), Phys. Rev. **D88**, 11, 112006 (2013), [arXiv:1310.3675].
- [271] G. Aad et al. (ATLAS), Eur. Phys. J. C 82, 7, 606 (2022), [arXiv:2201.02472].
- [272] G. Aad et al. (ATLAS), JHEP **2306**, 158 (2023), [arXiv:2205.06013].
- [273] A. Hayrapetyan et al. (CMS), Phys. Rev. D 109, 7, 072007 (2024), [arXiv:2309.16823].
- [274] LEP2 SUSY Working Group, ALEPH, DELPHI, L3 and OPAL experiments, note LEPSUSYWG/02-05.1, http://lepsusy.web.cern.ch/lepsusy.
- [275] V. Khachatryan et al. (CMS), Eur. Phys. J. C75, 7, 325 (2015), [arXiv:1502.02522].

- [276] T. Aaltonen et al. (CDF), Phys. Rev. **D88**, 3, 031103 (2013), [arXiv:1307.0474].
- [277] A. M. Sirunyan et al. (CMS), Phys. Rev. D 100, 11, 112003 (2019), [arXiv:1909.06166].
- [278] V. M. Abazov et al. (D0), Phys. Rev. Lett. 101, 111802 (2008), [arXiv:0806.2223].
- [279] G. Aad et al. (ATLAS), Phys. Rev. **D90**, 11, 112005 (2014), [arXiv:1409.5542].
- [280] G. Aad et al. (ATLAS), JHEP 12, 081 (2023), [arXiv:2307.14759].
- [281] O. Buchmueller et al., Eur. Phys. J. C71, 1722 (2011), [arXiv:1106.2529].
- [282] E. A. Baltz and P. Gondolo, JHEP 10, 052 (2004), [hep-ph/0407039].
- [283] B. C. Allanach and C. G. Lester, Phys. Rev. **D73**, 015013 (2006), [hep-ph/0507283].
- [284] R. Ruiz de Austri, R. Trotta and L. Roszkowski, JHEP **05**, 002 (2006), [hep-ph/0602028].
- [285] R. Lafaye et al., Eur. Phys. J. C54, 617 (2008), [arXiv:0709.3985].
- [286] M. Shaposhnikov, JHEP **08**, 008 (2008), [arXiv:0804.4542].
- [287] R. Trotta et al., JHEP 12, 024 (2008), [arXiv:0809.3792].
- [288] P. Bechtle et al., Eur. Phys. J. C66, 215 (2010), [arXiv:0907.2589].
- [289] E. Bagnaschi et al., Eur. Phys. J. C 78, 256, 1 (2018).
- [290] J. Costa et al., Eur. Phys. J. C 78, 158, 1 (2018).
- [291] E. Bagnaschi et al., Eur. Phys. J. C77, 4, 268 (2017), [arXiv:1612.05210].
- [292] E. Bagnaschi et al., Eur. Phys. J. C77, 2, 104 (2017), [arXiv:1610.10084].
- [293] L. A. Harland-Lang, V. A. Khoze and M. G. Ryskin, Eur. Phys. J. C76, 1, 9 (2016), [arXiv:1508.02718].
- [294] E. A. Bagnaschi et al., Eur. Phys. J. C75, 500 (2015), [arXiv:1508.01173].
- [295] O. Buchmueller et al., Eur. Phys. J. C74, 12, 3212 (2014), [arXiv:1408.4060].
- [296] M. Citron et al., Phys. Rev. **D87**, 3, 036012 (2013), [arXiv:1212.2886].
- [297] F. Ambrogi et al., Eur. Phys. J. C 78, 3, 215 (2018), [arXiv:1707.09036].
- [298] E. Bagnaschi et al., Eur. Phys. J. C 79, 2, 149 (2019), [arXiv:1810.10905].
- [299] A. Arbey et al., Phys. Rev. D 106, 5, 055002 (2022), [arXiv:2201.00070].
- [300] Supersymmetry Physics Results, ATLAS experiment, http://twiki.cern.ch/twiki/bin/view/AtlasPublic/SupersymmetryPublicResults/.
- [301] Supersymmetry Physics Results, CMS experiment, http://cms-results.web.cern.ch/cms-results/public-results/publications/SUS/index.html.